belspo

BRAIN-be

Belgian Research Action through Interdisciplinary Networks

PIONEER PROJECTS

IMPROVING KNOWLEDGE OF THE AMAZON RAINFOREST EMISSIONS (IKARE)

CONTRACT - BR/154/PI/IKARE

FINAL REPORT

17/09/2019

Promotors
Corinne Vigouroux, Royal Belgian Institute for Space Aeronomy (BIRA-IASB), 3 avenue Circulaire, B-1180 Brussels

Authors
Corinne Vigouroux, BIRA-IASB
Bart Dils, BIRA-IASB
Carlos Augusto Bauer Aquino, Instituto Federal de Educação, Ciência e Tecnologia de Rondônia (IFRO)
Christian Hermans, BIRA-IASB
Minqiang Zhou, BIRA-IASB
Bavo Langerock, BIRA-IASB
Trissevgeni Stavrakou, BIRA-IASB
Martine De Mazière, BIRA-IASB

IASI data have been provided by B. Franco (ULB) and OMI and TROPOMI data by I. De Smedt (BIRA-ISAB)

.be

Published in 2019 by the Belgian Science Policy Office
WTC III
Simon Bolivarlaan 30 boulevard Simon Bolivar
B-1000 Brussels
Belgium
Tel: +32 (0)2 238 34 11
http://www.belspo.be

Contact person: Georges JAMART
+32 (0)2 238 36 90

Corinne Vigouroux, B. Dils, C. A. Bauer Aquino, C. Hermans, M. Zhou, Bavo Langerock, T Stavrakou, M. De Mazière. Improving Knowledge of the Amazon Rainforest Emission (IKARE). Final Report. Brussels: Belgian Science Policy Office 2019 – 58 p. (BRAIN-be - Belgian Research Action through Interdisciplinary Networks)

TABLE OF CONTENTS

SUMMARY

Context

The Amazonian rainforest has a significant impact on air quality via the emission of biogenic volatile organic compounds (VOC) which are responsible for the photochemical production of ozone and other atmospheric oxidants. The deforestation has exacerbated the fire occurrences in this region, which impacts climate change via the release of carbon (CO_2, CH_4, CO, VOC, …) in the atmosphere. While the rate of deforestation has been decreasing and/or kept relatively stable between 2004 and 2015 (http://www.obt.inpe.br/OBT/assuntos/programas/amazonia/prodes), this 2019 year features intense biomass burning and was especially in the media spotlight (see WEB 2019 in the Sect. References below), due to an August month where the number of fires that was detected was more than doubled compared to August 2018.

Despite the impact of the Amazon region on climate change and human health, ground-based measurements of the atmospheric composition over the region are very sparse; in particular, there are no remote sensing measurements of VOC. There is a crucial need, in particular for model and satellite validation, of such ground-based data in Amazonia (e.g. Barkley et al., 2013). Indeed the atmospheric columns provided by ground-based remote sensing techniques are more comparable to satellite quantities and less subject to local pollution than in situ surface data.

This lead us to propose the measurements of such key atmospheric species at the very strategic site of Porto Velho (8.8°S, 63.9°W), Brazil, at the edge of the Amazon rainforest.
We relied on the strong expertise in remote sensing Fourier Transform InfraRed (FTIR) solar absorption measurements and data analysis (Senten et al., 2008; Vigouroux et al., 2009; Vigouroux et al., 2012), that we acquired at the Reunion Island, in the Indian Ocean. At this latter location, we are operating FTIR instruments in the frame of the NDACC (Network for the Detection of Atmospheric Composition Change) since 2002.

At both Reunion Island and Porto Velho, the measurements are automated and remotely controlled at BIRA-IASB. However, for the installation and maintenance of our instruments at Porto Velho, we have benefited from the collaboration with Luciana Gatti (Sao Paulo) through the project Belgian-Brazilian network for studying the Atmosphere above the Amazonian Forest (BAAF, Cooperation agreement BL/35/FWI09), and from our local partner Carlos Augusto Bauer Aquino (IFRO).

In the IKARE project, we proposed to focus on the analysis of selected key atmospheric species, to improve our knowledge of the Amazon rainforest emissions. These species are:

- three biogenic VOC: formaldehyde (HCHO), methanol (CH_3OH), and formic acid (HCOOH). These species are also emitted by biomass burning.

- three important biomass burning products: carbon monoxide (CO), ethane (C_2H_6) and hydrogen cyanide (HCN).

However, due to technical issues, no measurements of methanol and acid formic were possible until very recently (mid-June 2019). We therefore have added the biomass burning species C_2H_2 to this project.

These seven species are designated as the 'IKARE species' hereinafter.

Objectives

The first objective was to optimize the spectra measurements for the cloudy conditions at Porto Velho. One of the main challenges of the new location at Porto Velho are the cloudy conditions, especially during the rainy season (November-April). The remote sensing FTIR technique consists of solar absorption spectral measurements, therefore if clouds are present in the line of sight between the instrument and the sun, during the recording of a spectrum, the measurement can be corrupted and should be discarded. The first objective was to determine if morel measurements can be retained by either reducing the single measurement duration or using of a DC recording of the spectra (in which the detector signal is not high-pass filtered prior to digitization) instead of the current AC recording (where a high-pass filter is used). Both techniques lead to a lower precision of the measurements. The objective was therefore to choose the option that will provide the best compromise between the number of spectra and the measurement precision.

The second objective was to provide optimized retrieval strategies for the IKARE species under very humid conditions. Retrieval strategies have been successfully developed in the past at Reunion Island for all the IKARE species (Vigouroux et al., 2009; Vigouroux et al., 2012). This includes the choice of the spectral micro-window(s) used in the retrieval, which is a compromise between the strengths of the target gas absorption lines and those of the interfering species. Too strong interfering lines could mask the target gas signatures especially when these are weak as is the case for the IKARE species. This would impact the uncertainty of the retrieved target species. In the case of Porto Velho, which is a low altitude site in the tropics, the level of humidity is even higher (annual mean of 85%) than at Reunion Island (68%). Therefore, the interferences with the water vapour lines will be stronger there. The second objective was to check if adjustments of the retrieval strategies obtained for Reunion lsland are necessary to minimize the impact of water vapour interferences on the target gas retrievals.

The third objective was to obtain the IKARE species time-series (total columns and low vertical resolution profiles) at Porto Velho and their associated averaging kernels and uncertainty budgets, and to study their seasonal cycles and day-to-day variability. For formaldehyde, which has a short lifetime of 2-3 hours, the diurnal cycle can also be obtained. No clear diurnal cycle was observed at Reunion Island for the other IKARE species, even for the one with the shortest lifetime (HCOOH, 3 days). We checked if a diurnal cycle can be observed at Porto Velho, which is much closer to the emission sources. The two years duration of the IKARE project, did not allow us to propose a dedicated validation of satellite data; the objective here was to merely

provide and archive unique time series that are available for the satellite communities. However, due to the limited time-series that we obtained due to instrumental and custom problems, we decided to shift some allocated time from the 4th and 5th objective (see further) towards the comparisons with OMI and TROPOMI (HCHO), and IASI (CO, C_2H_2, CH_3OH, HCOOH).

The fourth objective was to evaluate the IMAGES model input parameters by making comparisons with our FTIR data (all species except HCN, which is not provided by IMAGES). We aim to improve the current knowledge in the Amazon rainforest emissions by evaluating the databases used by current models (fire emission database GFED4, anthropogenic database EDGAR, biogenic emissions of CH_3OH and HCOOH, emission ratios of biomass burning species,…).

The fifth objective was to explore the impact of different vegetation sources on the atmospheric composition at Porto Velho and to derive emission ratios of the biomass burning species. The goal here was to separate the data according to different air mass trajectories as calculated by the Lagrangian transport model Flexpart and to gain knowledge of the principal source regions influencing our measurements at Porto Velho. This established, differentiating the measurements as a function of vegetation source, can tell us more about the emission ratios for said type.

The longer-term objective is to start long-term monitoring at Porto Velho and to certify this site as a new NDACC station, for increasing the spatial coverage and significance of the network and the role of BIRA-ISAB at the international level.

Conclusions

While we have experienced many delays due to technical and custom problems, we can still state that the project has successfully reached its main objectives.

We have recorded one year of data (July 2016-July 2017) in the spectral region of HCHO, CO, C_2H_6, and HCN original IKARE species. At the time of this report, we have recorded **three months of data** (**mid June 2019-mid September 2019**) in the complete NDACC FTIR configuration (including spectral region for CH_3OH and HCOOH). The measurements are ongoing and are planned to continue as long as possible given our available funding.

We have optimized the retrieval settings of the six proposed IKARE species (HCHO, CO, C_2H_6, HCN, CH_3OH, and HCOOH) and of C_2H_2, according to the high humidity conditions of Porto Velho. The optimized HCHO settings have been published and are now used at more than 20 FTIR stations around the world (Vigouroux et al., 2018). They have also been used in Sun et al. (2018), which describes FTIR measurements in highly polluted areas in China.

We have obtained and studied the time-series of the seven IKARE species: the seasonal variability due to the intense biomass burning season in August-September is clearly observed in all the species available during the 2016 season (HCHO, CO, C_2H_6, HCN, and C_2H_2). And all the IKARE species (including the recent CH_3OH and HCOOH data) also show a strong increase in the August month, due to the very intense fires this 2019 year, as highly discussed in the media (see WEB 2019 references below). We observe monthly mean values larger by 30% to more than 50% (depending on the species) in August 2019 compared to August 2016. The day-to-day variability shows a clear correlation of the biomass burning tracer CO with the other IKARE species. We observe a small diurnal cycle in the HCHO data. While no clear diurnal cycle was observed at the remote site Reunion Island for CH_3OH and HCOOH, we do observe one for these two species at Porto Velho, a site nearby the emissions, for the period mid-June-July.

We have compared our FTIR data with satellite data. The HCHO comparisons show a negative bias for both OMI (-28%) and TROPOMI (-37%). Both satellites use similar algorithms (De Smedt et al. 2018) and, similar biases are thus expected. However to understand why TROPOMI has an even lower bias than OMI requires further investigation (De Smedt, private communication). The high negative bias at Porto Velho (a site with high HCHO concentrations) confirms our current validation study (under the Belspo funded project TROVA-2) using about 20 FTIR sites: the mean bias at all stations was -15%, with the largest negative biases (-24 to -46%) observed at polluted sites (Paris, Xianghe, Mexico City). Porto Velho will be included in the next ESA S5P validation report.

The validation of IASI data shows more contrasted results: while the comparisons of CO show a very good agreement, with a very low bias of -0.5% and a correlation coefficient of 0.90, the IASI C_2H_2 is much higher (+98%) than our FTIR measurements at Porto Velho. This IASI C_2H_2 data set is still under development and this first validation shows that more research is required in order to understand the high bias at Porto Velho. We cannot quantitatively compare CH_3OH and HCOOH from IASI and FTIR data yet, because our FTIR data starts in June 2019, while the currently available IASI data sets reach up to 2018 only. However, comparing our June-July data (which show e.g. similar values in 2016 and 2019 for the other IKARE species), we can see that IASI is biased low for both species, but much more for HCOOH (-58%) than for CH_3OH (27%).

We have compared our FTIR data with the IMAGES model data, for species measured in 2016-2017: HCHO, CO, C_2H_6, and C_2H_2 (model data for 2019 are not yet available, and HCN is not provided by IMAGES). Our comparisons show an overestimation of the model for all these four species (from 26% to 42% depending on the species), during the biomass burning season. This points to a likely overestimation of the burned material in the fire emission database used in the model (GFED4) during the August-September 2016 months, and/or to too large emission factors of all the species in the model. We have compared the enhancement ratios that we can obtain from the correlation slope between CO and our three other species to the enhancement ratios used in the IMAGES model (coming from the current literature for tropical forest). We found that

the model ones are indeed larger than the FTIR ones (by a factor of 2). More years of comparisons will help to quantify the respective contribution of emissions factors (constant values) and amounts of burned materials in GFED4.

The overestimation of the IMAGES model HCHO with OMI is also observed but with a larger amplitude (T. Stavrakou, private communication), and the inversion of OMI for optimizing the model emissions leads then to an underestimation of the model compared to FTIR, in agreement with our observed negative bias of OMI. We believe that FTIR measurements could be used in inversion studies: the satellite known negative bias could be corrected prior to its inversion by models to avoid having underestimated emissions in the model, especially when a network of FTIR stations are used to consolidate the validation results.

Looking at the different seasonality of the biases, we found that the anthropogenic emission database used in the model (EDGARv.4.3.2), might be about 10% too low for C_2H_6 over South America. Also, a large underestimation of C_2H_2 by the model is observed in in November-June (62%). This is due to the fact the biofuel emissions, important in Brazil, are not reported in the anthropogenic emission database EDGARv.4.3.2 used in IMAGES.

We have successfully determined the main source areas influencing the site, its predominant transport pathways as well as the variability in time thereof using the Flexpart trajectory model. By far the consistently dominant source region (by vegetation type) is Tropical moist forest. This information was used in the interpretation of FTIR derived fire emission ratios. Unfortunately, given the limited timeframe analysed (and low variability in source regions) we could not select a subset of the data that would allow us to confidently explore the emission factors for other vegetation types such as savannah grasslands.

Also, while fair correlations between the 2016 fire season and Flexpart simulations were established, this correlation broke down almost completely for July 2017. Calculations of the latter were based on the preliminary GFEDv4.1 run which uses a simple scaling based on a climatology and measurements from MODIS. Our analysis suggest that this simple preliminary approach fails to fully capture the 2017 events. A reanalysis and further exploration of the Flexpart data when our time series expands is foreseen.

Keywords

Amazon rainforest; FTIR measurements; biogenic emissions; biomass burning; formaldehyde; VOC

RESUME

Contexte

La forêt amazonienne a un impact significatif sur la qualité de l'air de par l'émission de composés organiques volatils (COV) biogéniques qui sont responsables de la production photochimique de l'ozone et d'autres oxydants atmosphériques. La déforestation a exacerbé l'apparition des feux dans cette région, ce qui impacte le changement climatique par le rejet de carbone (CO_2, CH_4, CO, COV, …) dans l'atmosphère. Alors que le taux de déforestation a diminué et/ou est resté stable entre 2004 et 2015 (http://www.obt.inpe.br/OBT/assuntos/programas/amazonia/prodes), cette année 2019 a été spécialement médiatisée (voir les références WEB 2019 à la fin du document), à cause d'un mois d'Août où le nombre de feux détectés a plus que doublé en comparaison d' Août 2018.

Malgré l'impact de la région amazonienne sur le changement climatique et la santé publique, les mesures au sol de la composition atmosphérique dans cette région sont très rares ; en particulier, il n'y a pas de mesures de télédétection des COV. Il y a un besoin crucial, en particulier pour la validation des modèles et des satellites, de ce type de données au sol en Amazonie (voir par ex. Barkley et al., 2013). En effet, les colonnes atmosphériques mesurées par les techniques de télédétection au sol sont plus comparables aux quantités mesurées par les satellites et moins sujettes à la pollution locale que les données de surface in situ.

Cela nous a mené à proposer la mesure de ce type d'espèces atmosphériques clefs au site stratégique de Porto Velho (8.8°S, 63.9°O), Brésil, à la limite de la forêt amazonienne. Nous nous sommes appuyés sur notre grande expertise des mesures d'absorption solaire à Transformée de Fourier InfraRouge (FTIR) et de leur analyse (Senten et al., 2008; Vigouroux et al., 2009; Vigouroux et al., 2012), que nous avons acquise à L'Ile de La Réunion, dans l'Océan Indien. Depuis 2002, nous sommes responsables de mesures FTIR à La Réunion, dans le cadre du réseau international NDACC (Network for the Detection of Atmospheric Composition Change).

Aux deux sites La Réunion et Porto Velho, les mesures sont automatisées et contrôlées à distance à BIRA-IASB. Mais, pour l'installation et la maintenance de nos instruments à Porot Velho, nous avons bénéficier de la collaboration avec Luciana Gatti (Sao Paulo) à travers le projet « Belgian-Brazilian network for studying the Atmosphere above the Amazonian Forest » (BAAF, accord de coopération BL/35/FWI09), et avec notre partenaire local Carlos Augusto Bauer Aquino (IFRO).

Dans le projet IKARE, nous avons proposé de nous focaliser sur l'analyse d'espèces atmosphériques clefs, pour améliorer notre connaissance des émissions de la forêt amazonienne. Ces espèces sont:

- trois COV biogéniques : le formaldéhyde (HCHO), le méthanol (CH_3OH), et l'acide formique. Ces espèces sont aussi émises par les feux de biomasse.
- trois importants produits de feux de biomasse: le monoxyde de carbone (CO), l'éthane (C_2H_6) et le cyanure d'hydrogène (HCN).

Mais, à cause de problèmes techniques, les mesures de méthanol et d'acide formique n'ont été possible que depuis très récemment (mid-June 2019). Nous avons alors ajouté, dans le courant du projet, l'espèce de feux de biomasse C_2H_2.

A partir d'ici, ces sept espèces sont désignées comme étant les "espèces IKARE".

Objectifs

Le premier objectif était d'optimiser les mesures de spectres pour les conditions nuageuses de Porto Velho. Un des challenges principaux du nouveau site de Porto Velho sont les conditions nuageuses, surtout pendant la saison des pluies (Novembre-Avril). La technique FTIR consiste dans des mesures d'absorption spectrale solaire. De ce fait, si des nuages sont présents dans la ligne de mire entre l'instrument et le soleil pendant l'enregistrement d'un spectre, celui-ci peut être corrompu et doit être rejeté. Le premier objectif était de déterminer si des mesures supplémentaires peuvent être sauvées, soit en réduisant la durée d'une mesure soit en utilisant l'enregistrement DC des spectres (dans lequel le signal du détecteur n'est pas filtré à l'aide d'un filtre passe-haut avant la numérisation) à la place de l'actuel enregistrement AC (où un filtre passe-haut est utilisé). Ces options conduisent toutes les deux à une moins bonne précision des mesures. L'objectif était donc de choisir l'option qui conduirait au meilleur compromis entre le nombre de spectres et la précision des mesures.

Le second objectif était d'établir des stratégies d'inversion optimisées pour les espèces IKARE dans des conditions de grande humidité. Les stratégies d'inversion ont été développées avec succès dans le passé pour La Réunion pour toutes les espèces IKARE (Vigouroux et al., 2009; Vigouroux et al., 2012). Ceci inclut le choix des micro-fenêtres spectrales utilisées dans l'inversion, qui est un compromis entre les intensités des raies d'absorption de l'espèce ciblée et celles des espèces interférentes. Des raies interférentes trop intenses pourraient masquer les signatures des espèces ciblées, surtout quand celles-ci sont faibles, ce qui est le cas des espèces IKARE. Ceci impacterait l'incertitude sur l'inversion des espèces ciblées. Dans le cas de Porto Velho, qui est un site à basse altitude dans les tropiques, le niveau d'humidité est encore plus grand (moyenne annuelle de 85%) qu'à La Réunion (68%). Les interférences avec les raies de vapeur d'eau seront donc plus fortes là-bas. Le second objectif était de vérifier si des ajustements des stratégies d'inversion obtenues pour La Réunion sont nécessaires pour minimiser l'impact des interférences avec les raies de vapeur d'eau sur les inversions des espèces ciblées.

Le troisième objectif était d'obtenir les séries temporelles des espèces IKARE (colonnes totales et profils à basse résolution verticale) à Porto Velho et leurs fonctions de moyennage associées ainsi que leur budget d'erreur, et d'étudier leur cycle saisonnier et leur variabilité journalière. Pour le formaldéhyde, qui a un court temps de vie de 2-3 heures, le cycle diurne peut aussi être

observé. Aucun cycle diurne n'a été observé à La Réunion pour les autres espèces IKARE, même pour celle ayant le temps de vie le plus court (HCOOH, 3 jours). Nous avons étudié si un cycle diurne pouvait être observé à Porto Velho, qui est beaucoup plus près des sources d'émissions. La durée limitée de deux ans du projet IKARE ne nous avait pas permis de proposer une validation des données satellites. Mais, dû aux séries temporelles limitées que nous avons obtenues à cause de problèmes instrumentaux et douaniers, nous avons décidé d'accorder du temps, initialement alloué aux 4ème et 5ème objectifs, aux comparaisons avec les satellites OMI et TROPOMI (HCHO), et IASI (CO, C_2H_2, CH_3OH, HCOOH).

Le quatrième objectif était d'évaluer les paramètres d'entrée du model IMAGES en faisant des comparaisons avec nos données FTIR (toutes les espèces IKARE sauf le HCN, qui n'est pas fourni par IMAGES). Nous voulons améliorer la connaissance actuelle des émissions de la forêt amazonienne en évaluant les bases de données utilisées par les modèles (bases de données des feux GFED4 et d'émissions anthropiques EDGAR, les émissions biogéniques de CH_3OH et HCOOH, les rapport d'émissions des espèces de feux de biomasse,…).

Le cinquième objectif était d'explorer l'impact des différentes sources de végétation sur la composition atmosphérique à Porto Velho et d'obtenir les rapport d'émissions des espèces de feux de biomasse. Le but était de séparer les données en fonction des différentes trajectoires des masses d'air calculées par le modèle de transport Lagrangien Flexpart, et de déterminer les principales régions sources influençant nos mesures à Porto Velho. Ceci établi, différencier les mesures suivant la source de végétation peut nous en dire plus sur les rapports d'émissions suivant le type de végétation.

L'objectif à long terme de ce projet est de continuer les observations à Porto Velho dans le futur et de certifier ce site comme une nouvelle station du réseau NDACC, pour améliorer la couverture spatiale et l'importance de ce réseau ainsi que le rôle de BIRA-IASB au niveau international.

Conclusions

Alors que nous avons dû subir beaucoup de délais à cause de problèmes techniques et douaniers, nous pouvons tout de même affirmer que ce projet a atteint avec succès ses objectifs principaux.

Nous avons mesuré un an de données (Juillet 2016 – Juillet 2017) dans la région spectrale des espèces IKARE originellement proposées: HCHO, CO, C_2H_6, and HCN. Au moment d'écrire ce rapport, nous avons enregistré **trois mois de données (mi-Juin 2019 – mi-Septembre 2019)** dans la configuration complète du réseau NDACC (ce qui inclut la région spectrale de CH_3OH et HCOOH). **Les mesures continuent** et nous souhaitons les poursuivre aussi longtemps que le permet notre financement.

Nous avons optimisé les stratégies d'inversion des six espèces IKARE proposées (HCHO, CO, C_2H_6, HCN, CH_3OH, and HCOOH) et de C_2H_2, en tenant compte du grand taux d'humidité de Porto Velho. La stratégie d'inversion de HCHO a été publiée et est maintenant utilisée par plus de 20 stations FTIR dans le monde (Vigouroux et al., 2018). Elle a aussi été utilisée dans Sun et al. (2018).

Nous avons obtenu et étudié les séries temporelles des sept espèces IKARE: la variation saisonnière due à la saison de feux de biomasse intenses en Août-Septembre est clairement observée pour toutes les espèces disponibles durant la saison 2016 (HCHO, CO, C_2H_6, HCN, and C_2H_2). Et toutes les espèces IKARE (incluant les données très récentes de CH_3OH et HCOOH) montrent également une très forte augmentation ce mois d'Août, liée aux feux très intenses cette année 2019, comme abondement relayé par la presse (voir les références WEB 2019). Nous observons des valeurs mensuelles moyennes de 30 à plus de 50% (suivant les espèces) plus grandes en Août 2019 comparées à Août 2016. La variabilité journalière montre clairement une corrélation entre le traceur de feux de biomasse CO et les autres espèces IKARE.

Nous observons un faible cycle diurne dans les données du HCHO. Alors qu'aucun cycle diurne n'avait été observé clairement pour le CH_3OH et le HCOOH à La Réunion, nous en observons un pour ces deux espèces à Porto Velho, un site proche des émissions, pour la période mi-Juin-Juillet.

Nous avons comparé nos données FTIR à des données satellite. Les comparaisons de HCHO montrent un biais négatif de OMI (-28%) et de TROPOMI (-37%). Les deux satellites utilisant un algorithme similaire (De Smedt et al. 2018), des biais similaires sont effectivement attendus. Quoiqu'il en soit, plus d'investigation est nécessaire pour comprendre pourquoi TROPOMI est encore plus bas qu'OMI (De Smedt I., communication privée). Le grand biais négatif à ce site de Porto Velho où les niveaux de HCHO sont élevés confirme notre étude actuelle de validation de TROPOMI (dans le cadre du projet financé par Belspo TROVA-2) utilisant environ 20 sites FTIR : le biais moyen pour toutes les stations est de -15%, avec les biais négatifs les plus importants observés pour les stations très polluées (Paris, Xianghe, Mexico). Le site de Porto Velho sera inclus dans le prochain rapport de validation ESA S5P. La validation d'IASI montre des résultats plus contrastés : alors que les comparaisons du CO montrent un excellent accord, avec un très petit biais de -0.5% et un coefficient de corrélation de 0.90, le C_2H_2 d'IASI est beaucoup plus haut (+98%) que nos mesures FTIR à Porto Velho. Ce produit C_2H_2 d'IASI est toujours en développement et cette première validation montre qu'il faut poursuivre les recherches afin de comprendre ce grand biais à Porto Velho. Nous ne pouvons pas comparer quantitativement CH_3OH et HCOOH d'IASI à nos données FTIR qui ne commencent qu'en 2019, ces données IASI ne nous en étant fournies pour l'instant que jusqu'en 2018. Mais, en comparant les données de Juin-Juillet (des valeurs similaires entre 2016 et 2019 sont observes pour les autres espèces IKARE à ces mois-ci), nous observons qu'IASI a un biais négatif pour les 2 espèces, bien que plus grand pour HCOOH (-58%) que pour CH_3OH (-27%).

Nous avons comparé nos données FTIR avec le modèle IMAGES, pour les espèces mesurées en 2016-2017: HCHO, CO, C_2H_6, et C_2H_2 (les données 2019 du modèle ne sont encore disponibles, et

HCN n'est pas fourni par le modèle). Nos comparaisons montrent une surestimation du modèle pour ces quatre espèces (de 26% à 42% suivant l'espèce) pendant la saison des feux de biomasse. Cela montre qu'il y a probablement une surestimation de la quantité de matériel brûlé dans la base de données utilisée dans le modèle (GFED4) pendant les mois d'Août-Septembre 2016, et/ou que les facteurs d'émission de ces espèces sont trop grands dans le modèle. Nous avons comparé les rapports d'émissions que nous pouvons obtenir à partir des pentes de corrélation entre le CO et les autres trois espèces avec ceux utilisés dans le modèle IMAGES (venant de la littérature actuelle pour les forêts tropicales). Nous avons trouvé que ceux du modèle sont effectivement plus grands que ceux venant des mesures FTIR (d'un facteur 2). Plus d'années de comparaisons nous aideront à quantifier les contributions respectives des facteurs d'émissions (valeurs constantes) et les quantités de matériel brûlé dans GFED4.

La surestimation du HCHO dans le modèle IMAGES est aussi observée lors de comparaisons avec OMI, mais avec une amplitude plus grande encore (T. Stavrakou, communication privée), et l'inversion des données OMI pour l'optimisation des émissions du modèle conduit alors à une sous-estimation du modèle par rapport au FTIR, en accord avec le biais négatif d'OMI observé avec les données FTIR. Nous pensons que nos données pourraient être utilisées dans des études d'inversion: par exemple, le biais négatif connu d'OMI et TROPOMI en comparant avec les données FTIR pourrait être corrigé pour éviter d'obtenir des émissions sous-estimées dans le modèle, particulièrement quand un réseau de stations FTIR est utilisé pour consolider les résultats de validation.

En regardant la différente saisonnalité des biais, nous avons trouvé que la base de données d'émissions anthropiques utilisée dans le modèle (EDGARv.4.3.2), pourrait être 10% trop basse pour C_2H_6 en Amérique de Sud. Une grand sous-estimation du C_2H_2 par le modèle est observée en Novembre-Juin (62%). Ceci est dû au fait que les émissions de biocarburant, importantes au Brésil, ne sont pas incluses dans la base de données d'émissions anthropiques EDGARv.4.3.2 utilisée dans IMAGES (T. Stavrakou, communication privée).

Nous avons déterminé avec succès les régions sources principales influençant le site de Porto Velho, les voies de transport dominantes ainsi que leur variabilité en utilisant le modèle de trajectoire Flexpart. La région source dominante (par type de végétation) est, de loin, la forêt tropicale humide. Cette information a été utilisée dans l'interprétation des rapports d'émissions dérivés des mesures FTIR. Malheureusement, étant donné la période limitée de mesures (et la faible variabilité des régions sources), nous n'avons pas pu sélectionner un sous-ensemble de données qui nous aurait permis d'obtenir les facteurs d'émissions pour d'autres types de végétation comme la savane. Aussi, alors que des corrélations raisonnables entre le FTIR et les simulations de Flexpart sont observées pendant la saison des feux 2016, cette corrélation s'effondre en Juillet 2017. Les calculs pour 2017 étaient basés sur une version préliminaire de GFEDv4.1 qui utilise une simple mise à l'échelle à partir d'une climatologie et de mesures de MODIS. Notre analyse suggère que cette simple approche préliminaire ne réussit pas à capturer les évènements de 2017. Une ré-analyse et une exploitation supplémentaire des données Flexpart quand notre série temporelle sera plus longue est prévue.

Mots-clés

Forêt amazonienne; mesures FTIR; émissions biogéniques; feux de biomasse; formaldéhyde; COV

1. INTRODUCTION

The Amazon rainforest has a significant impact on air quality and climate change via the emission of biogenic volatile organic compounds (VOCs) and the release of carbon (CO_2, CH_4, CO, VOC,...) in the atmosphere by biomass burning. However, despite the crucial need of ground-based data in this region of high environmental interest, the measurements are very sparse; in particular, there are no remote sensing measurements of VOC emitted by the rainforest.

In addition to their own scientific value, the ground-based remote sensing techniques are perfectly suited for satellite validation because they measure comparable quantities (i.e. integrated total columns of atmospheric species) and are less subject to local pollution than in situ surface data. The satellite community is calling for such ground-based measurements over Amazonia (e.g. Barkley et al., 2013; De Smedt et al., 2015). For example, ground-based measurements of formaldehyde, which has a short lifetime of 2-3 hours, can provide its diurnal cycle, which is not possible from current satellite measurements (e.g. GOME-2 measures only at about 9:30 local time, and OMI at 13:30). Since an important negative bias is observed between OMI and GOME-2 HCHO total columns above Amazonia (De Smedt et al., 2015), the ground-based observations can provide more insight to conclude whether this bias is due to the diurnal cycle or to satellite uncertainties.

Another direct application of ground-based measurements is the model validation and improvement as done in the past with Reunion Island data. Indeed, the underestimation of HCHO by the model IMAGES (Vigouroux et al., 2009) has questioned the model parameter inputs (OH concentrations, fire injection heights and convective updraft fluxes, as well as the Global Fire Emission Database GFED2). The comparisons with the other IKARE species at Reunion Island showed that GFED3 underestimates the pyrogenic emissions in this region (Vigouroux et al., 2012). Also, while satellite global data are very useful for source inversion studies, as made in Stavrakou et al. (2011) for methanol and Stavrakou et al. (2012) and Paulot et al. (2011) for formic acid, the comparisons with ground-based data are crucial in such analysis to validate or constrain the inversion results. E.g., we observed that the a posteriori emissions of methanol derived from IASI inversions above Reunion Island are too low during the fire season, suggesting that IASI may underestimate CH_3OH in this situation.

Based on our strong expertise in FTIR measurements at BIRA-IASB, we have successfully installed and are still operating a Fourier Transform Infra-Red (FTIR) spectrometer at Porto Velho, a strategic location in the Amazon region, in Brazil. Due to technical issues with the instrument and custom problems, we have experienced delays and interruptions in the planned measurements. However, we are able to provide unique data series of five key VOCs and biomass burning products for the period July 2016-July 2017 (HCHO, CO, HCN, C_2H_6, C_2H_2), and from June 2019 to present for the seven IKARE species (including CH_3OH and HCOOH). With one year of data, we are able to show the seasonal variability observed at Porto Velho for the four measured species, with a maximum during the biomass burning season (August-September). The time-series improve the knowledge of the day-to-day and

seasonal variability of the Amazonia emissions but also of the diurnal cycle of short-lived species, such as formaldehyde, which is not provided by current satellites. Our very recent measurements in August 2019 allow the detection of the intense fires over Amazonia extensively discussed in the media, with monthly mean columns of CO, C_2H_6, HCN, and C_2H_2 about 30 to 50% larger in August 2019 compared to August 2016. Large column values are also observed in our recent CH_3OH and HCOOH August 2019 measurements.

The HCHO data after June 2019 are used for the validation of TROPOMI S5P data (Belspo project TROVA-2, TROPOMI launched in autumn 2018). We also show in this report, as an illustration of the future use of our data, the comparison of HCHO with OMI data for the whole period of measurement, and the comparisons of CO, C_2H_2, CH_3OH and HCOOH with IASI time-series.

We have compared our species with the IMAGES model data, and we show in this report that some emission parameters for biomass burning seem to be overestimated in the model, while the anthropogenic emissions are too low in the model, especially for C_2H_2.

We have investigated, via transport modelling, the predominant transport pathways and source regions that impact our measurements at Porto Velho. It is shown that these pathways show a consistent pattern will little variation, controlled by the position of the Inter Tropical Convergence Zone (ITCZ). By far the consistently dominant source region (by vegetation type) is Tropical moist forest.

2. METHODOLOGY AND RESULTS

In this section, we will go through the work packages (WPs), and present together the methodology and main results.

2.1. WP1: Optimization of the spectra measurements

- **Task 1.1 Maintenance of the spectrometer (C. Hermans and Carlos Aquino)**

Monitoring by remote control of the proper functioning of the instruments is carried out daily from Brussels, in addition to the on-site supervision by our Brazilian colleague Carlos Aquino. The data is transferred by FTP every night and a first quality control (signal-to-noise ratio) is performed automatically with an alarm signal in case of drift.

The maintenance and supply (nitrogen liquid, ...) is carried out by Carlos Aquino. In case of major maintenance we can interact with the communication systems that we have (Phone calls, skype sessions, webcam, remote control) for solving together instrumental problems.

Two major maintenances took place for the period **between July 2016 and July 2017**:

1- One of the two motors of the sun-tracker broke down which stopped measurements during 2 months, Dec. 2016 and Jan. 2017, the time necessary to the purchase of a replacement in Belgium, clear customs formalities, and transport it to Porto Velho.

2- The air compressor also had to be changed (it is used to open and close the sun-tracker according to the weather, and to provide dry air). We were able to buy a new compressor in Brazil. And we found a solution for the air dryer system connected to the compressor. We were only able to solve this problem by June 2017. Since dry air is required for MCT detector measurements, which are needed for the detection of CH_3OH and HCOOH, these 2 species could not be measured before the last visit to the instrument by Cristian Hermans (BIRA-IASB), in June 2019.

In July 2017, a vibration appeared on the scanner level of the 125M spectrometer (Bruker). This vibration was not easy to understand even for Bruker's engineers. Nevertheless, after a thorough study, Bruker found a solution that asked for the purchase of equipment (upgrade eddy-current retarder) and the arrival of an engineer on site in Porto Velho for the installation. **The Bruker engineer and the new equipment were available only in October 2018**, more than one year after the problem had arised. This slow response from Bruker was/is also an issue in the whole NDACC IRWG (InfraRed Working Group) community, and an official letter has been sent to the Bruker company in the name of the IRWG to solve this in future collaboration.

When restarting the entire installation in October 2018, one of the sun tracker motor had failed (azimuth motor). After the purchase of this motor and its replacement on site, which required again a time delay due to the Brazilian customs, **the measurements resumed in June 2019** in its complete configuration (two detectors (InSb and MCT for the near and medium IR).

In summary, we have recorded one year of data (July 2016-July 2017) for the HCHO, CO, C_2H_6, and HCN original IKARE species, and for the additional C_2H_2 species. At the time of this report, we have exploited one month of data (mid June 2019-mid July 2019) for the whole set of IKARE species (including CH_3OH and HCOOH). The measurements are ongoing and are planned to continue as long as possible given our available funding.

- **Task 1.2 Adjustment of the BARCOS system (M. Zhou, C. Hermans and C. Vigouroux)**

One of the main challenges of the new location at Porto Velho are the cloudy conditions, especially during the rainy season (November-April): if clouds are present in the line of sight between the instrument and the sun during the measurement of a spectra, it can be corrupted and should be discarded. The usual configuration is to record a single spectrum after the

averaging of 4 or 6 individual scans (a scan corresponds to moving the mirror of one arm of the interferometer along the optical path). This averaging allows for an enhanced signal-to-noise ratio (SNR) of the spectrum. If the sun intensity varies too much (threshold is set at 5%) during the recording time of the whole spectrum (few minutes), the spectrum is rejected.

We give in Fig. 1 the statistics, for each month, of the number of recorded spectra at Porto Velho and Maïdo (left panel) and the percentage of the rejected spectra at both stations (right panel).

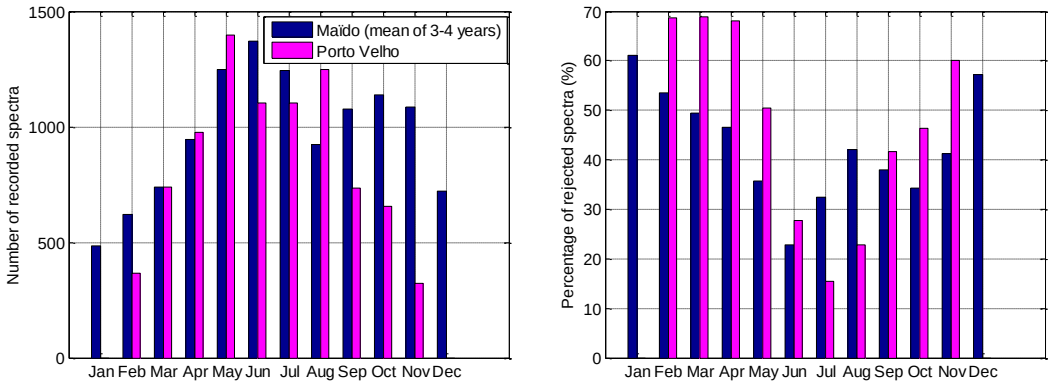

Figure 1: Number of total recorded spectra and percentage of rejected spectra per month at Maïdo and Porto Velho.

A spectral measurement starts and a spectrum is recorded if the sun appears with enough intensity. Figure 1 (left panel) shows that at Maïdo the number of recorded spectra is the lowest during the Dec-March period (in agreement with the rainy season at Reunion Island) while at Porto Velho, the rainy season with less recorded spectra began already in September and lasted up to March. Note that the climatological rainy season in Porto Velho is October-May, but here we have only one year of measurements, so they might not be exactly representative. The lack of recorded spectra in Jan-Dec at Porto Velho is due to a sun-tracker failure (see Task 1.1), not the weather. The right panel of Fig. 1 shows the percentage of rejected spectra (number of spectra with intensity variation $>5\%$ i.e. clouds appearing during the record of the 4/6 scan spectra). As expected, during the rainy season, not only less spectra are recorded but, among those, more are rejected due to clouds, and we clearly see that the situation is worse at Porto Velho.

Two options were tested to reduce the number of rejected spectra. To save time on the project, knowing that the installation at Porto Velho had been delayed by about one year, we decided to make our tests on the Reunion Island spectra.

1) **The first test** is to adapt our measurement system (so-called BARCOS, Neefs et al. 2007) to record spectra for each scan separately. This will reduce the probability of having to eliminate because of cloud occurrences. The averaging of clear-sky scans,

to improve the SNR, will be done afterwards. We expect by this adaptation, for days with partial cloudiness, to save additional measurements.
For this exercise, we recorded at Maïdo, during 3-months (27 March to 29 June 2016), and only for a selected type of spectra (so-called "hh"), spectra with only 2 scans (one with the mirror moving forward and one moving backward to its initial position). The time to record one scan is 70.6 seconds. In total, 1296 spectra were collected during this period.
The interferogram contains one forward and one backward scan measured with only AC signal by the Bruker system (with a 20-40 kHz frequency). Each forward or backward scan can be analysed individually. In addition, the BARCOS system records the DC signal with a low temporal resolution (about 3 seconds).

Selecting a good scan:
Based on the BARCOS DC signal (IRDC) and the Bruker only AC interferogram (IFG), four criteria are used to identify the good scan:

- The ratio of the standard deviation of the IRDC to the maximum of the IRDC is less than 8%;
- The ratio of the median of the IRDC to the maximum of the IRDC is larger than 90%;
- The relative difference between the maximum and minimum around the zero optical path difference (ZOPD) is less than 20%;
- The absolute value of the IFG at ZOPD is larger than 0.05.

Averaging the good scans:
Averaging the good scans reduces the white noise of the spectrum. However, we cannot average too many spectra, since the solar zenith angle of each spectrum (therefore the sounded air masses for which we look for the species concentration) is changing due to their different measurement time. According to the old settings (6 scans for hh spectra), we average all the good scans within a 6-scans time window.

Table 1 shows the increase in spectra when relaxing the 6-scan threshold (first row) towards 2; with each step progressively including the remaining spectra. In total 84 averaged spectra have less than 6 good scans: **indeed the number of good spectra increases if we allow to average only 2 scans of the remaining scans (from 132 to 216), but with a quite large reduction of the SNR.**
In Task 1.3, we study the impact of the SNR on the quality of the species retrievals, in order to decide if 2 or 4 scans is enough, or if we have to keep our previous approach (e.g. one spectra "hh" = average of 6 scans).

Table 1: The number and SNR of the averaged spectra with 2 to 6 good scans.

Number of good scans	Number of averaged spectra	SNR (Mean/std)
6	132	1263/57
5	3	1053/9
4	22	1030/17
3	6	895/38
2	53	732/17

2) **In the second test**, we wanted to follow the approach of using the DC recording to correct the interferograms for the solar irradiance variation (SIV) due to clouds, as done within TCCON (Total Carbon Column Observing Network) and explained in Keppel-Aleks et al. (2007). This would have allowed us (i) to reject less spectra by increasing the threshold of sun variability up to at least 10%, and (ii) to increase the quality of the spectra after correction (Keppel-Aleks et al., 2007). The DC recording is currently not used in the NDACC community because it has the disadvantage of decreasing the SNR of the interferograms.

We wanted to adapt our current AC configuration to the AC+DC configuration which requires an update to the BARCOS electronic system, and choose the option that would provide the best compromise between the number of spectra and their SNR. However**, this requires the purchase and installation of a high speed acquisition board and important modifications to the acquisition software that can only be made on-site by our BIRA experts. This would require more time than we can afford**, especially with the one-year delay of the installation.

Therefore, we tried to reconstruct the AC+DC signal with the Bruker only AC interferogram and the BARCOS IRDC signal (low temporal resolution). Figure 2 shows an example of the IRDC, interferogram and resulting spectrum in case of a large variation of the solar irradiance during the scan because of cloud occurrences. We can see that the AC signal is seriously influenced by the SIV because many spikes are present in the interferogram (middle panel). **As the AC part is contaminated, it is not possible to do the DC correction based on the Bruker AC signal and the BARCOS IRDC signal.**

In conclusion, for this project, the DC signal cannot be used to reduce the SIV impact on the interferogram. An installation of high speed acquisition board could be done, but in the future only.

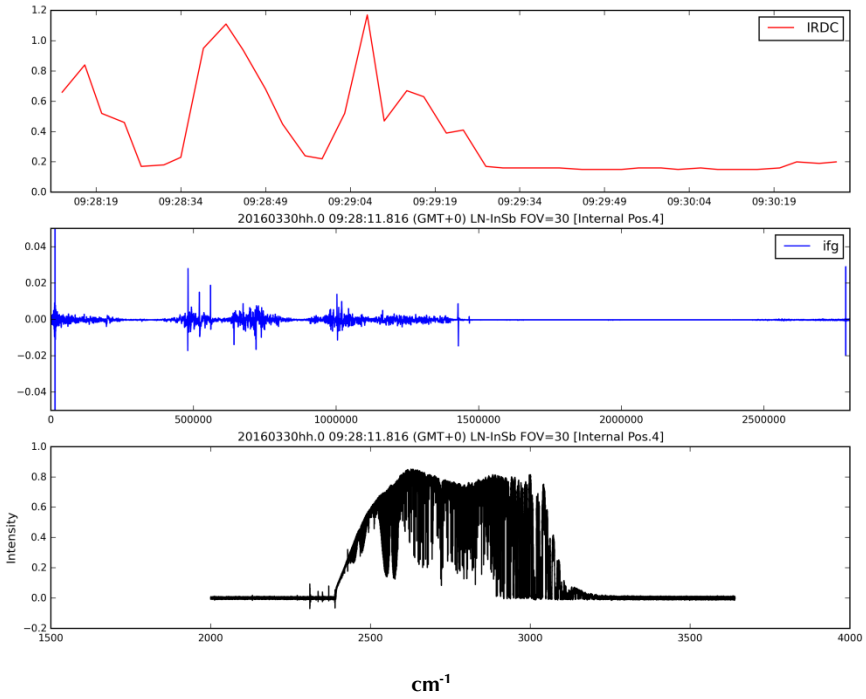

Figure 2: One typical case when the solar brightness showed large variation (i.e. under cloudiness condition). BARCOS IRDC signal (upper panel); Bruker only AC interferogram (middle panel); FTIR spectrum (bottom panel).

- **Task 1.3 Choosing the best measurement approach (all)**

The SNR is proportional to the square root of the number of scans (Table 1) and the precision on the retrieved columns of the target species is related to the SNR. Therefore, a compromise is needed between the number of available spectrum (e.g in our test case between 132 high SNR spectra; 132+ 25 medium SNR; or 132 + 25 + 59 low SNR; see Table 1). If the low and/or medium SNR is not sufficient to retrieve our species with a good precision, then we will keep using our previous strategy: a single spectra is an average of 6 scans. We therefore made the retrievals of HCHO during these 3 months of test at Maïdo. We chose this species due to its small absorption signature which makes the SNR a crucial parameter in its detection. For this study, we use separately all available 2 scans spectra (including breaking up the 6-scan high SNR spectra: 132*3 + 25*2+59) as measured during the March-June 2016 period, and compare the retrieval results with the ones obtained when 4 and 6 scans averaging can be made. Figure 3 shows the SNR obtained for the different averaged spectra (2 / 4 / 6), the resulted RMS (root mean square = the residuals of the fit), and the HCHO total columns. While the RMS are increased by using only 2 scans measurements, they are still below the limit of 0.4 that we usually use for HCHO retrievals during our routine work. We see also that the HCHO columns look similar in the 3 cases, but with a larger dispersion for the 2 scans spectra, which means that the random noise error is indeed larger for the 2 scans retrievals. Indeed, the mean random error on the HCHO columns is increasing with

decreasing number of scan: from 2.0E14 molec/cm^2 (6 scans), to 2.2E14 molec/cm^2 (2 scans), therefore the random error is degraded by 10% using 2 scans spectra.

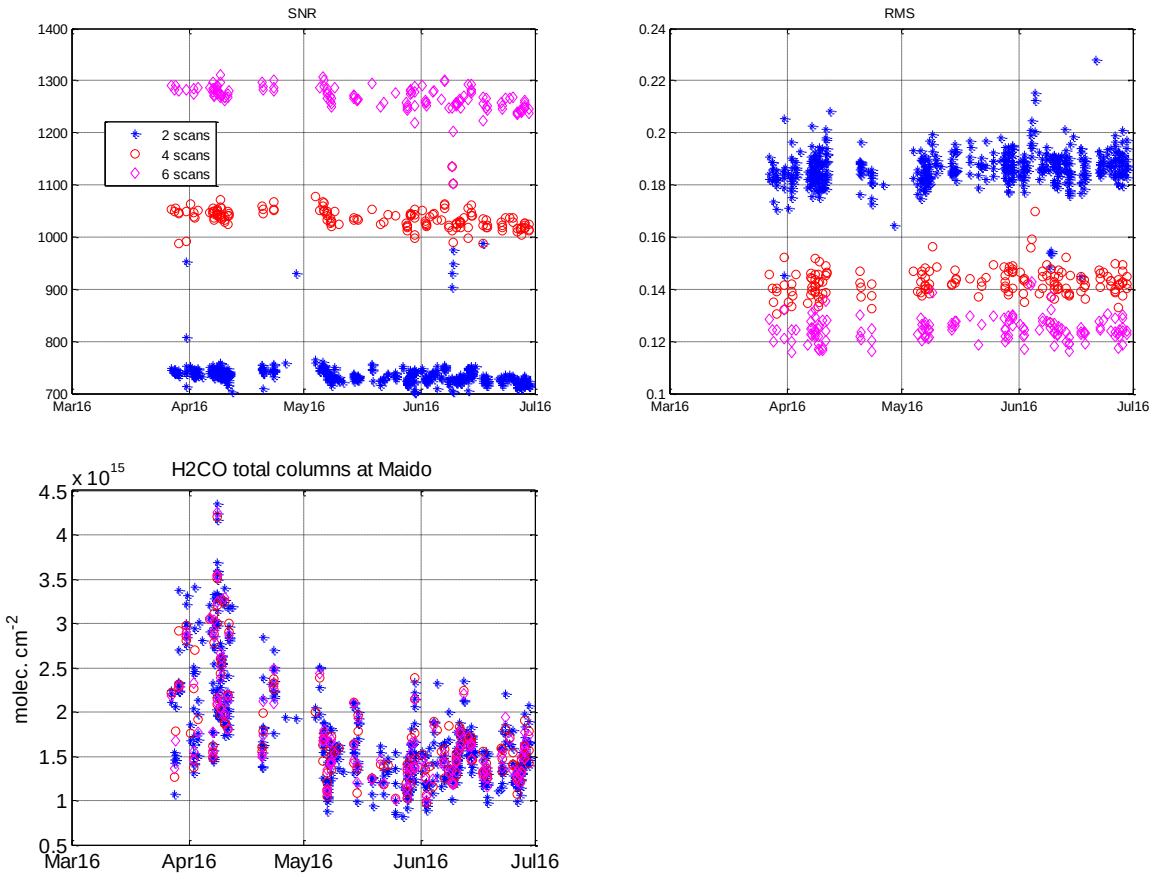

Figure 3: SNR, RMS and HCHO total columns for the test period at Maïdo, for 2 (blue), 4 (red), and 6 (magenta) scans spectra.

This analysis was made with Maïdo spectra, because of the one year delay on the installation of the instrument. **They looked promising due to the still low RMS obtained with the 2 scans spectra, and the reasonable decrease of 10% on the associated random error budget compared to the 6 scans spectra.**

However, when Porto Velho spectra became available, we observed that the RMS with the 6 scans spectra (mean = 0.19) are already providing an RMS similar to the 2 scans spectra at Maïdo (see Fig. 3), and a larger random error (3.4E14 molec/cm^2). The reasons are the inferior quality of the instrument at Porto Velho (Bruker 125M) compared to the one at Maïdo (Bruker 125HR), and the higher level of humidity at the ground station Porto Velho, leading to more interference with water vapour lines in the spectra. **In those conditions, to avoid a further degradation of the random error, we have chosen to keep the 6 scans approach at Porto Velho.**

2.2. WP2: Optimization of the retrieval strategies of IKARE species

- **Common parameters for all the IKARE species:**

- The a priori profiles for all species, except for H_2O and its isotopologues, are taken from the model WACCMv6. Single a priori profiles are used for each molecule for the whole period of measurements: they correspond to the mean of the calculated species profiles at the location of PortoVelho during the period 1980-2020.

- Due to the high variability of H_2O and its isotopologues and the presence of their intense lines which are interfering with the target IKARE species lines in the fitted mws, especially in the case of the very humid site of Porto Velho, we use specific a priori H_2O (and isotopologues) profiles for each spectra. They are coming from the 6-hourly files provided by NCEP (National Centers for Environmental Prediction).

- **Task 2.1: HCHO retrieval strategy**

The retrieval strategy of formaldehyde (HCHO) has been revisited. The starting point was our previous work published in Vigouroux et al. (2009). The main changes are the fitted micro-windows (mws). The **atm16 spectroscopy** allow to enlarge the mws without having bad residuals (that were mainly due to CH_4 lines that were not correct in the HITRAN 2008 database used in Vigouroux et al., 2009). This new line list has been constructed by from Geoff Toon (JPL, USA), starting from the HITRAN 2012 database. When some line parameters from HITRAN 2012 are found not good (i.e. are giving large residuals when the spectra are fitted), they are replaced by ad-hoc parameters determined by G. Toon. This is the case for some O_3, CH_4, and HDO lines that are present in the chosen mws. Having larger mws is important for HCHO since its spectral signatures are quite small and wide. We have sent our optimized settings to the international IRWG community of NDACC in order to obtain a large network of stations measuring HCHO in view of the TROPOMI upcoming validation (project ESA NIDFORVal, funded by Belspo with the project TROVA). **Our improved retrieval settings are now successfully used by more than 20 FTIR stations, and have been published in Vigouroux et al. (2018).**

- **Task 2.2: CO retrieval strategy**

CO, C_2H_6 and HCN are primary target gases of the NDACC IRWG. As such, it is preferable for a harmonization of the NDACC products that all stations used as similar settings as possible. It can happen, as we experienced this for our other site St-Denis at Reunion Island, that NDACC settings are not good in case of very humid sites, because of too large H_2O interferences.
For CO, the **recommended NDACC mws** (2069.56-2069.76; 2157.50-2159.15; 2157.78-2157.89 cm^{-1}) and a priori profiles from WACCMv6 appeared to give good results for Porto

Velho. Therefore, we only had to optimize the regularization to obtain good CO time-series at this humid site, as we did for St-Denis.
Concerning the spectroscopy, we used the previous version **atm12 for the CO lines** because it gave slightly better residuals than the atm16 version or HITRAN 2008.

- **Task 2.3: C_2H_6 retrieval strategy**

For C_2H_6, a network effort for harmonization within NDACC was led by E. Mahieu (from ULg, Belgium). We managed to follow his settings at Porto Velho and Reunion Island, except for one of the mws (2986.50-2986.85 89 cm^{-1}) that has to be skipped because it is too contaminated by H_2O. The two remaining mws are **2976.660-2977.059 and 2983.2-2983.6 cm^{-1}**. The C_2H_6 WACCMv6 a priori profiles had to be scaled at all stations due to a too large underestimation of the model.
In this network harmonization, the same spectroscopy has to be used by all stations: the **pseudo line list from Geoff Toon (c2h6_2720_3100.101)** for C_2H_6 and HITRAN 2008 for interfering species.

- **Task 2.4: HCN retrieval strategy**

For HCN, we have tested our mws previously defined for StDenis and described in Vigouroux et al. (2012). In this previous work, only 2 of the 3 recommended NDACC mws are used due to too strong interference with H_2O in the 3rd one. At Porto Velho, we slightly reduce the size of the 1st mw, again to reduce the H_2O impact, and the final mws are: **3268.14-3268.35 and 3331.4-3331.8 cm^{-1}**. Some adaptation has been made in the regularization, and in the H_2O treatment (the $H_2{}^{17}O$ isotopologue profile is fitted simultaneously).
The recommended NDACC spectroscopy for HCN is HITRAN 2008, and it has been used in Vigouroux et al. (2012). However, at our very humid sites, we noticed that the use of **HITRAN 2012** significantly improved the residuals in the case of H_2O lines. To simplify, we use HITRAN 2012 for all gases in the HCN retrievals (for HCN, HITRAN 2012 = HITRAN 2008).
These new H_2O lines have a strong effect on the HCN columns themselves: they are higher by about 25%.

- **Task 2.5: CH_3OH retrieval strategy**

We could work on the CH_3OH and HCOOH retrievals only from mid-June 2019, when the MCT measurements became possible (see Task.1.1).
Fortunately, the previous settings used in Vigouroux et al. (2012) are also well suitable for Porto Velho conditions, and we can use the **1029.0-1037.0 cm^{-1}** mw.
Concerning the spectroscopy, we moved from HITRAN 2008 to HITTRAN 2012 for all species in this micro-window.

- **Task 2.6: HCOOH retrieval strategy**

For HCOOH, we used the **1102.75-1106.4 cm^{-1}** mw, as done at Reunion Island (Vigouroux et al., 2012). We also moved to HITRAN 2012.

- **Task 2.7 (additional task): C_2H_2 retrieval strategy**

As we did not have the MCT measurements up to very recently, we decided to work instead on another biomass burning species: C_2H_2. We used the same spectral signature as in Vigouroux et al. (2012) but with slightly different mw limits, which gave better residuals (again because of H_2O interferences): **3250.05-3251.02 cm^{-1}**.
We again moved to HITRAN 2012 for this species.

2.3. WP3: Retrieve and archive the data series of the IKARE species

- **Task 3.1: Time-series and variability of the IKARE species**

From WP2 retrieval strategies, we obtained a complete year of measurements for 4 of the 6 IKARE species: CO, C_2H_6, HCN and HCHO, and we provide the additional species C_2H_2 as well. **A clear seasonal variability is observed for the 5 species** (Fig. 4). The dominant source of these species at Porto Velho is biomass burning. For HCHO, secondary biogenic production is also a major contributor to the seasonal cycle. The uncertainties on the observed total columns are discussed in Task 3.2.

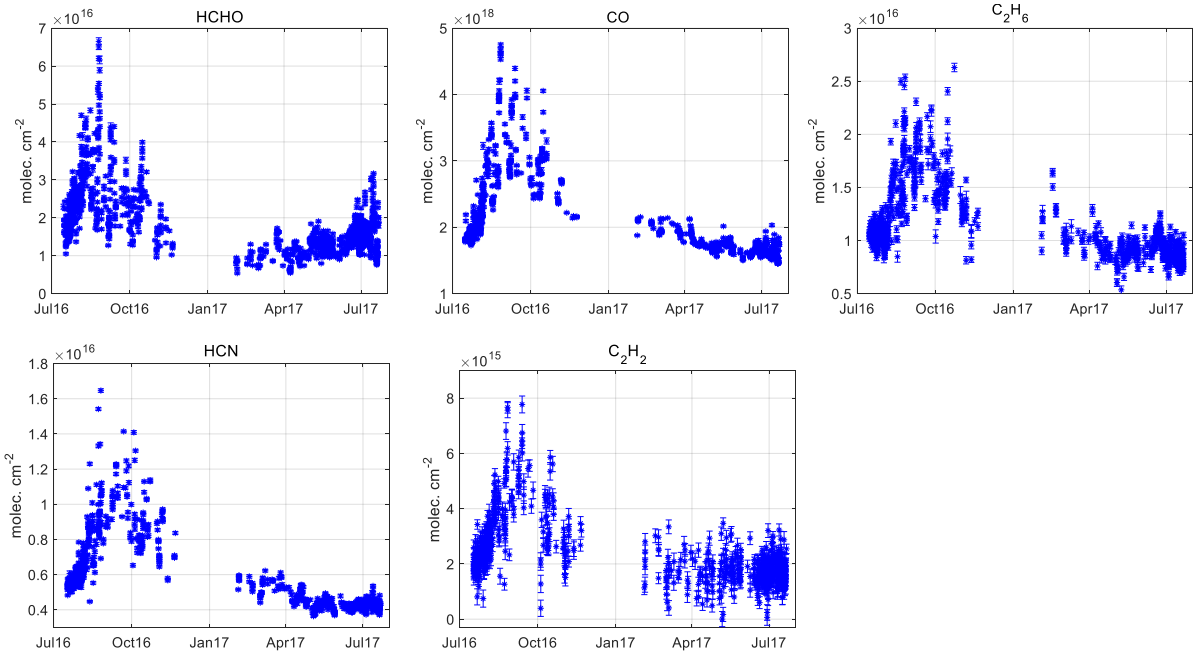

Figure 4: Total column time-series of HCHO, CO, C_2H_6, HCN, and C_2H_2 at Porto Velho **for the July 2016-July 2017 period**, from FTIR data. Since the systematic part always dominates the error budget (See Sect. 3.2), the error bars correspond here to the random uncertainties only, to highlight the precision of our measurements.

For CH_3OH and HCOOH, only few weeks of measurements are available up to now due to technical issues (see Task. 1.1), but the seasonal variability will be observed in the coming months. The 2019 observations at the time of this report are shown in Fig. 5 for the 7 species. We already see the high increase in August 2019 due to intense fires. As discussed in the public media, the August 2019 values are larger than the August 2016 period for all our biomass burning species. We show this inter-annual variability in Fig. 6. It will be interesting in the coming weeks to compare the September 2019 with the September 2016 values, in order to check if the total of biomass burned area has indeed increase for the whole fire period season, or if this is only a shift in the burned area (more in August, less in September).

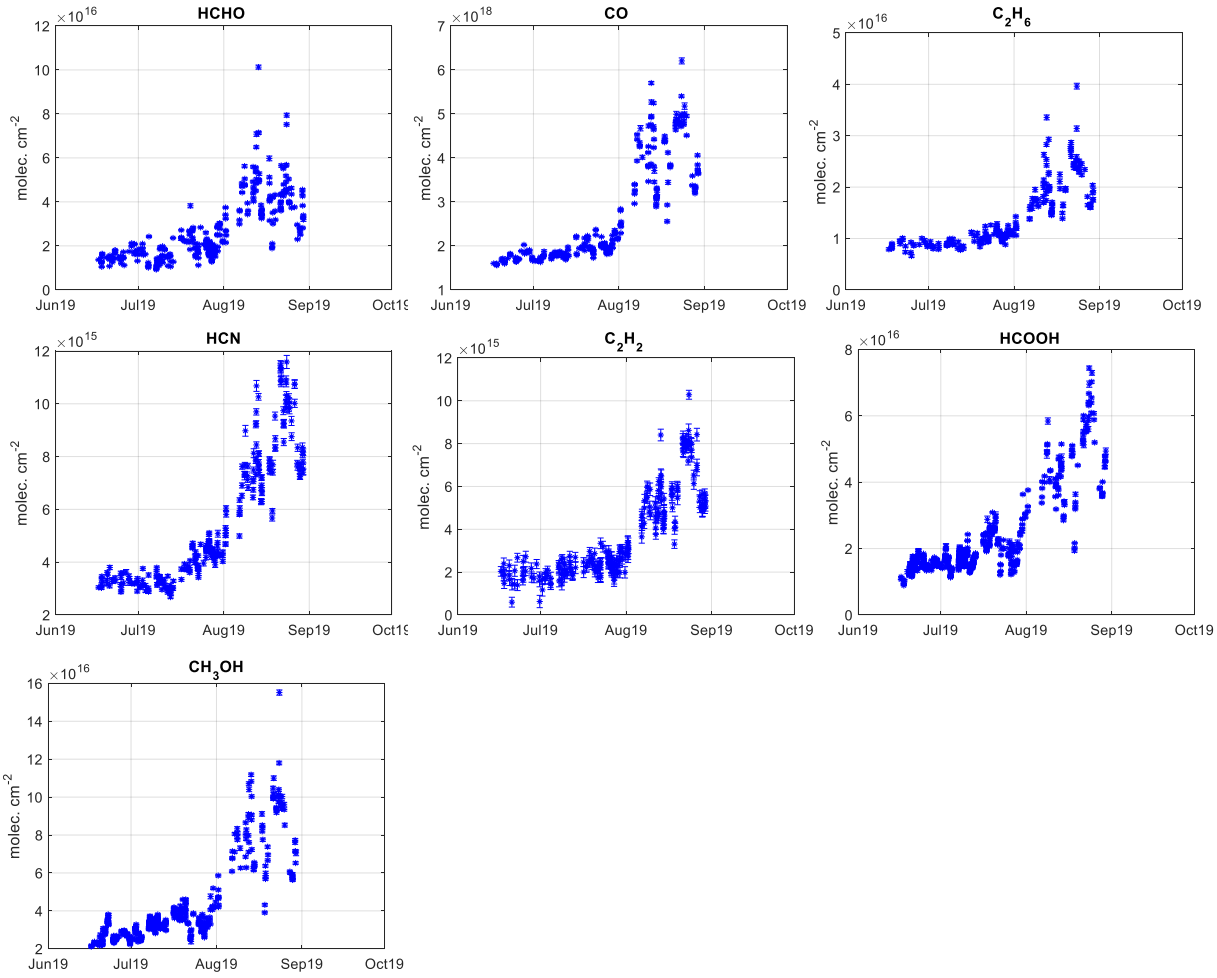

Figure 5: Total column time-series of HCHO, CO, C_2H_6, HCN, C_2H_2, CH_3OH, and HCOOH at Porto Velho for the **June 2019-August 2019** period, from FTIR data. The error bars correspond here to the random uncertainties.

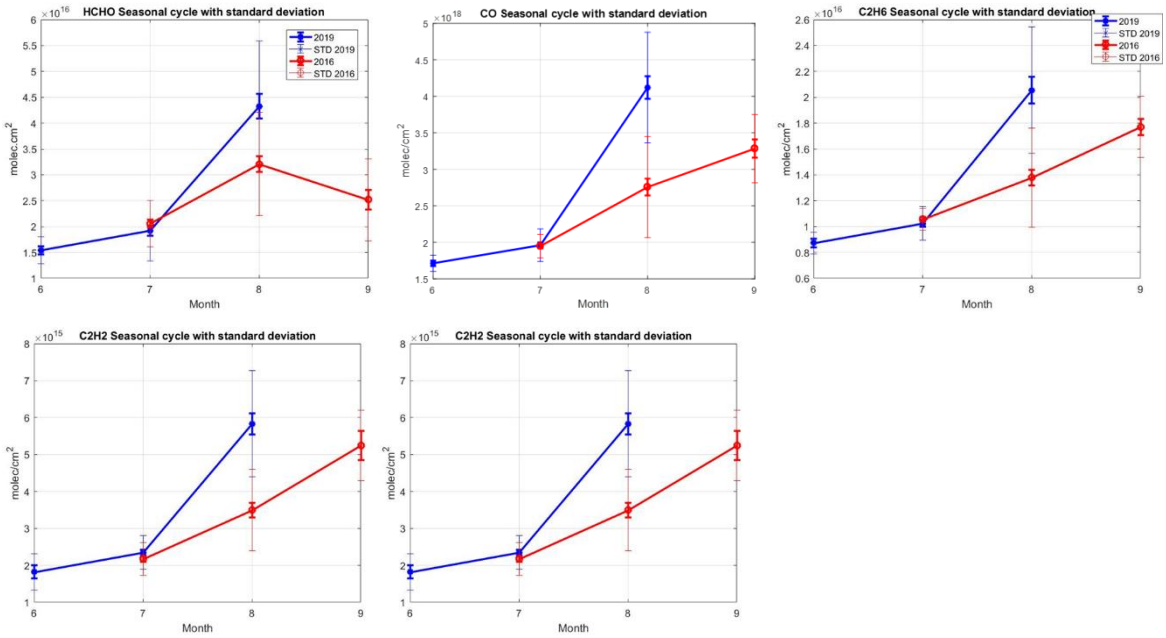

Figure 6: Comparison of the 2016 and 2019 monthly means, showing enhanced columns during the August 2019 intense fires.

Concerning the day-to-day variability, we find very good correlation between all the IKARE species (HCHO, C_2H_6, HCN, C_2H_2, HCOOH and CH_3OH) total columns with the "reference" biomass burning tracer CO (Fig. 7), confirming the common biomass burning sources of the observed species, and the good sensitivity of our measurements. The recent intense fires in August 2019 allow us to provide the correlation plots for CH_3OH and HCOOH as well.
The correlation plots can be used to derive emission ratios, as discussed in Sect. 2.4.

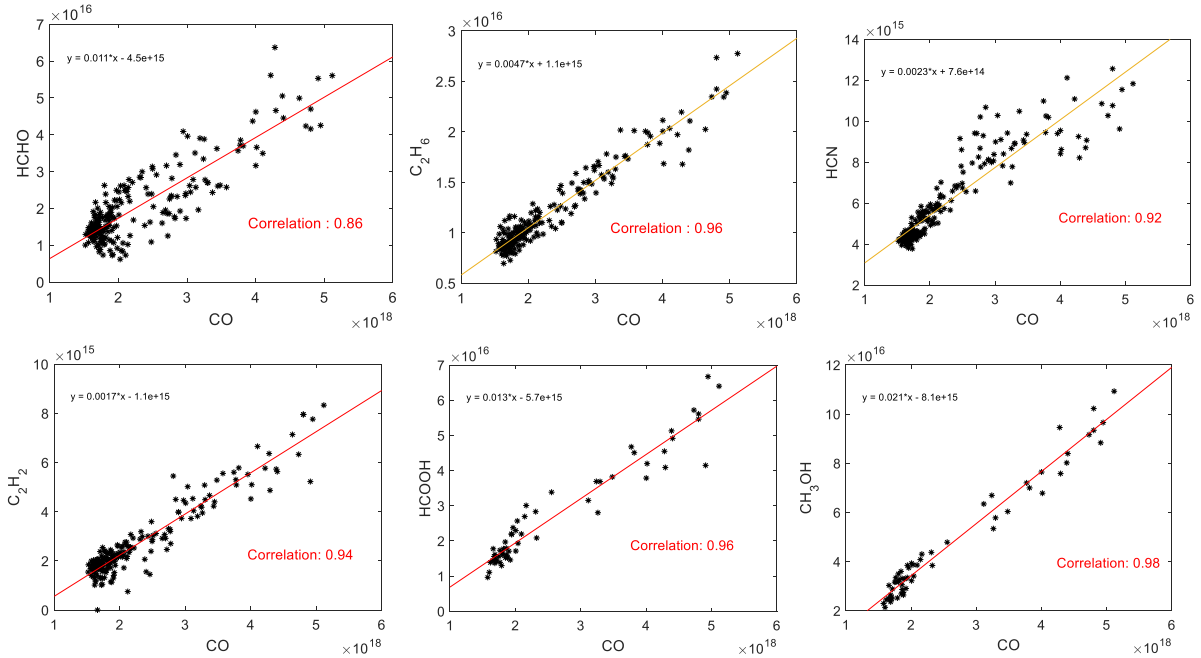

Figure 7: Correlation plots of daily means HCHO, C_2H_6, HCN, C_2H_2, HCOOH and CH_3OH with CO.

Diurnal variability:

We have explored the diurnal cycle of the IKARE species. Because of the strong seasonal cycle of these species (see Fig. 4), we look at the diurnal cycles at four seasons (Feb-Mar-Apr; May-Jun-Jul; Aug-Sep-Oct; Nov-Dec-Jan). As expected by the long lifetime of CO, C_2H_6, HCN, C_2H_2 (several months to several weeks), no clear diurnal cycle is observed for these four species (not shown). We show the diurnal cycle at local time in Fig. 8, for HCHO, CH_3OH and HCOOH.

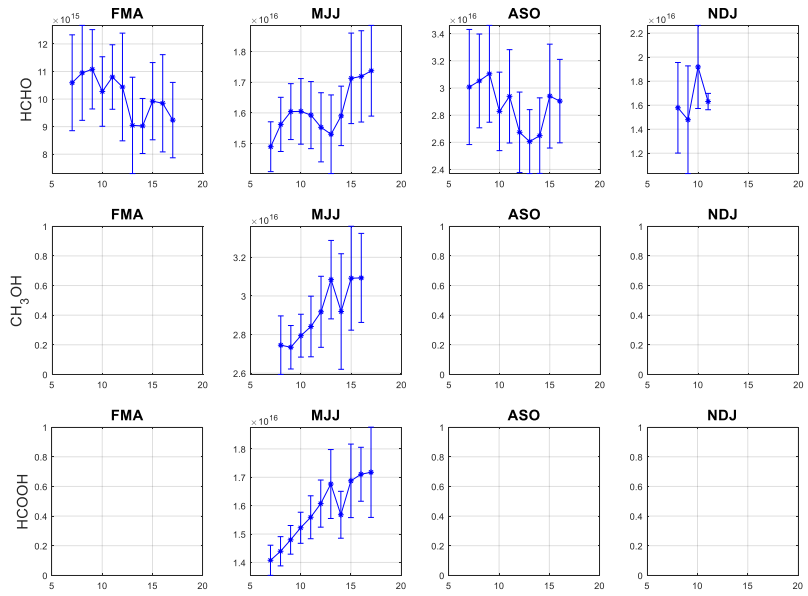

Figure 8: Diurnal cycle of the total columns (molec/cm^2) of HCHO, CH_3OH and HCOOH, in local time. The error bars are the standard deviations on the hourly means.

HCHO diurnal cycle:

The observed HCHO diurnal cycles at all seasons show about 2E15 molec.cm^2 difference between the maximum and minimum values, and are usually not significant because the standard deviations on the hourly means are quite large, even when we distinguish between the seasons. The morning values are larger than the afternoon ones during the Feb-Apr months, while it is the opposite during the May-July months. A minimum seems to occur around 1 pm in both cases, as well as in the Aug-Oct period. This diurnal cycle could explain partly the differences observed in Rondônia in De Smedt et al. (2015) between morning (SCIAMACHY; GOME-2A; GOME-2B; measuring around 9 and 9:30 am) and afternoon satellite (OMI; 1:30 pm). However, if the mean 2007-2013 difference between GOME-2A and OMI is important over Amazonia (about 4E15 molec.cm^2), the difference is quite variable depending on the year (their Fig. 15). Therefore, the GOME-2B and OMI differences should be quantified for the period of our FTIR measurements (2016-2017).

More measurements are probably needed to see if the HCHO diurnal cycle observed at present is really significant. **We plan in the coming months to increase the number of spectra recorded in the HCHO spectral region in order to better observe it.** This is at the

detriment of measuring other spectra types (therefore other retrieved species), so it should be done on a short duration basis.

CH_3OH diurnal cycle:

Although we have only one month of data at present, we clearly see an increase of CH_3OH during the day (Fig. 8) in the June-July period. This reflects the biogenic emissions of the rainforest, as already observed during the GABRIEL (Guyanas Atmosphere-Biosphere exchange and Radicals Intensive Experiment with the Learjet) airborne campaign in October 2005 (Eerdekens et al., 2009). We show in Fig. 9 their Fig. 8c for methanol diurnal cycle using the PTR-MS (Proton Transfer Re-action Mass Spectrometry) technique. We see in their observations a similar shape of the increase of methanol. The amplitude of the increase is much more pronounced in the airborne data (values are more than doubled) compared to FTIR (10-15% of increase), but this is expected since FTIR measures the total column amounts, so the effect of local emissions is diluted in the vertical averaging. Also the GABRIEL campaign took place in October during the dry season, therefore we need a few more months of measurements to better compare the diurnal cycles.
The ASO plot in Fig.8 reflects at present only the August 2019 month, with a lot of variability due to the intense fires this year, so this is also too soon to draw conclusions for this period.

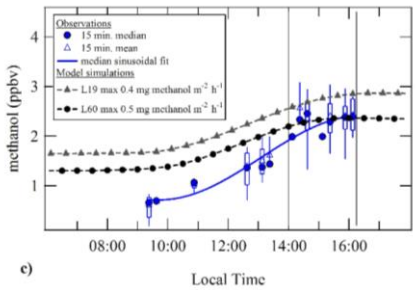

Figure 9: Methanol diurnal cycle obtained during the GABRIEL airborne campaign (Fig. 8c of Eerdekens et al., 2009)

HCOOH diurnal cycle:

The clearly observed HCOOH diurnal cycle, in Fig. 8, has a similar shape to CH_3OH, with a larger amplitude (20%). An increase during the day was also observed in Rondônia field measurements in both dry and wet season (Kuhn et al., 2002), with a larger amplitude during the dry one.

Our promising CH_3OH and HCOOH diurnal cycle results will be extended in the coming months to cover the different seasons.

- **Task 3.2: Uncertainties estimation**

  During the EUFP7 QA4ECV project we have aligned the uncertainty computation across the NDACC FTIR instruments. The SFIT4 retrieval software (used at BIRA and at many other FTIR

sites in the network) has been updated so that the output uncertainties are aligned with the other retrieval software used within NDACC. The error budget has been calculated for each species, following the formalism of Rodgers (2000) as done in e.g.Vigouroux et al. (2012), and is given in Table 2. The systematic uncertainty is quite variable among the IKARE species (from 2.6 to 32%) and is dominated by the spectroscopic uncertainties on the line intensity and the air pressure dependence of the line shape. The temperature and interfering species can also be contributing systematic error sources. The random uncertainties are usually small (0.9 to 2.8%), except for C_2H_2 (10.6%). The dominant contribution to the random error budget is the measurement noise. An empirical verification of our random error estimation is to check the difference between two adjacent measurements (taken within 35 minutes, assuming then that the difference is due to the precision of the measurement and not to the natural variability of the air masses and species). We give in Table 2 the median of these differences. We see that the empirical precision is usually close to the theoretical estimation (CO, HCOOH), or slightly larger. The latter case could be due to an underestimation of the random uncertainties or to the smoothing error which is not included in the usual error budget provided in NDACC files.

Table 2: Uncertainty budget for the IKARE species. The median of the difference between two adjacent measurements (within 35 minutes) and the mean DOFS are also given.

	Random uncertainty	Systematic uncertainty	Median difference within 35 minutes	Mean DOFS	Smoothing error	Total Random (Rand & Smoo)
HCHO	1.9 %	12.8 %	3.2 %	1.1	4.4%	4.8 %
CO	0.9 %	2.6 %	0.8 %	2.2	0.6 %	1.0 %
C_2H_6	2.8 %	10.3 %	4.9 %	1.3	11.7 %	11.4 %
HCN	1.3 %	21.4 %	2.2 %	1.5	21.4 %	21.4 %
C_2H_2	10.6 %	32.0 %	15.0 %	1.0	15.7 %	19.0%
CH_3OH	2.3 %	15.5 %	1.4 %	1.2	3.2 %	3.9 %
HCOOH	1.6 %	8.8 %	1.5 %	1.0	0.8 %	1.8 %

This smoothing error (reflecting the poor vertical resolution of our remote sensing technique), is not provided because its calculation requires the knowledge of the natural variability (covariance matrix) of the species profile (Rodgers and Connor, 2003), which is usually not (well) known.

We provide as an estimation, in Table 2, the smoothing error that can be calculated from the covariance matrix built from the WACCMv6 model profiles of each species at Porto Velho, and the total random uncertainty that can then be estimated (root sum square of random and smoothing errors). If we compare the total random error with the empirical precision estimation, it seems that the smoothing error calculated using the WACCMv6 covariance matrices are overestimated in some cases (HCN, C_2H_6).

The approach chosen within NDACC is to not include this smoothing error in the standard geoms files, but to provide the averaging kernel matrix (AK) associated to each measurement, from which the user can either: 1) calculate himself the smoothing error if a good covariance

matrix becomes available; 2) avoid this smoothing error calculation by using the AK to smooth the profile to be validated (model or satellite). We give in Fig. 10, the plots of the averaging kernels (rows of AK) of each species, and the total column averaging kernel as well. The degrees of freedom for signal (DOFS) are the trace of the AK and are given in Table 2. A value close to 1 means that we do not have vertical information, i.e., we can only measure the total column amounts, the retrieved profiles basically follow the a priori profile shape. Only for CO, 2 independent partial columns can be derived from our measurements. The total column averaging kernel indicates the altitude range where our measurements has some sensitivity: e.g. it can be seen from Fig. 10 that we are sensitive to a CO concentration change also near the ground, while for HCN the sensitivity is low in the lower troposphere.

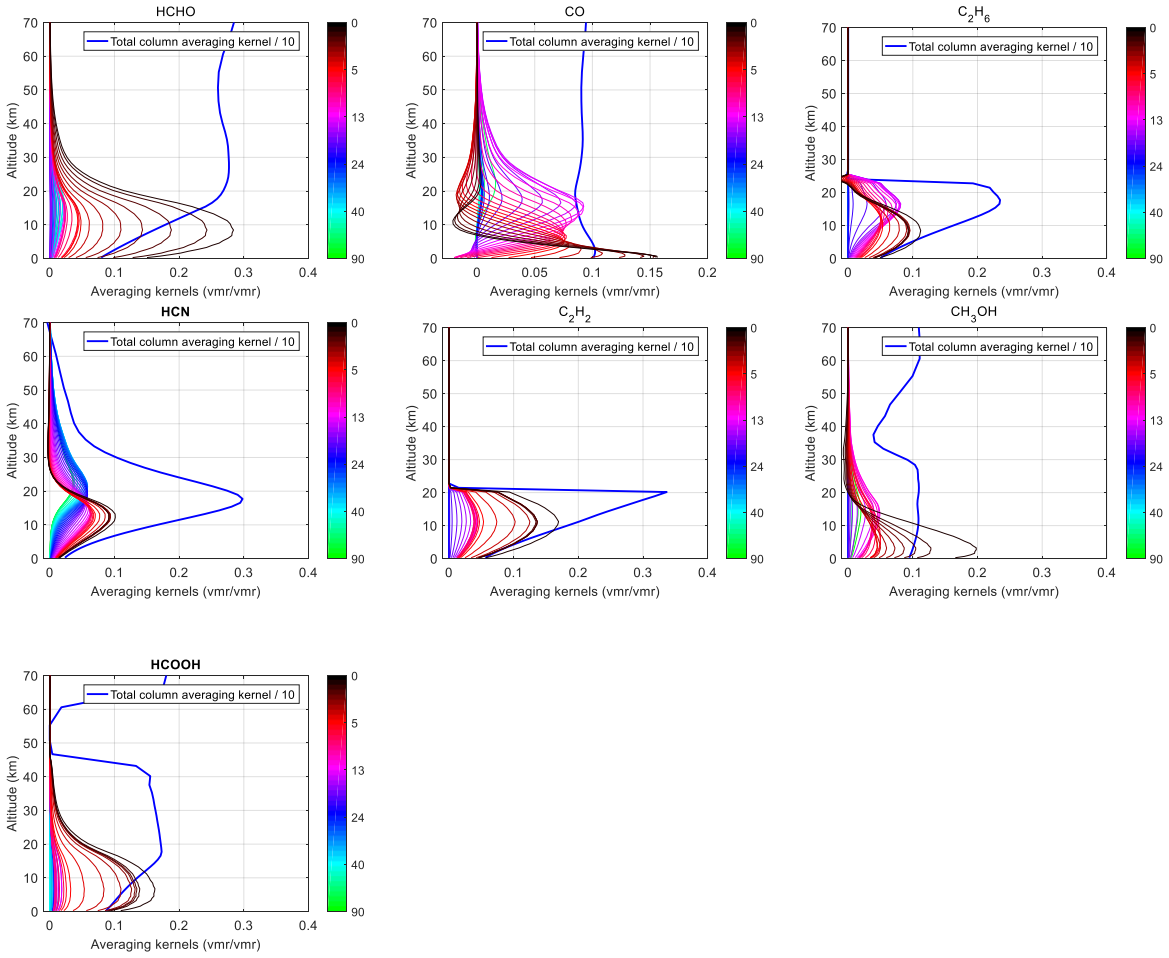

Figure 10: Averaging kernels of the IKARE species.

- **Task 3.3: Satellite validation** (additional task; not in initial project)

Although it is not part of the IKARE project, to highlight the future potential of our time-series, we compare our measurements with satellite data, when available (Fig. 11). The OMI and IASI Metop-B CO and C_2H_2 comparisons are made during the July 2016- July 2017

measurement period at Porto Velho, while the TROPOMI validation can only be made with our recent measurements (June-July 2019), since TROPOMI was launched in Autumn 2017. The CH_3OH and HCOOH measurements at Porto Velho are too recent to have satellite data available, but we still compare the levels with IASI data measured in the previous year.

OMI and TROPOMI HCHO validation:

The HCHO OMI data are from I. De Smedt (BIRA-ISAB). The OMI retrieval algorithm has been improved within the project Q44ECV, and has also been implemented for the TROPOMI retrievals (De Smedt et al., 2018). Although some OMI validation has been reported in conferences, using MAX-DOAS data (G. Pinardi, BIRA-IASB), **there is no published paper on this important improved QA4ECV data set. Using the HCHO FTIR network of stations that we built, a publication will be performed by I. De Smedt, and the Porto Velho site will be a key site due to very high levels of HCHO compared to other FTIR stations (Vigouroux et al., 2018).**

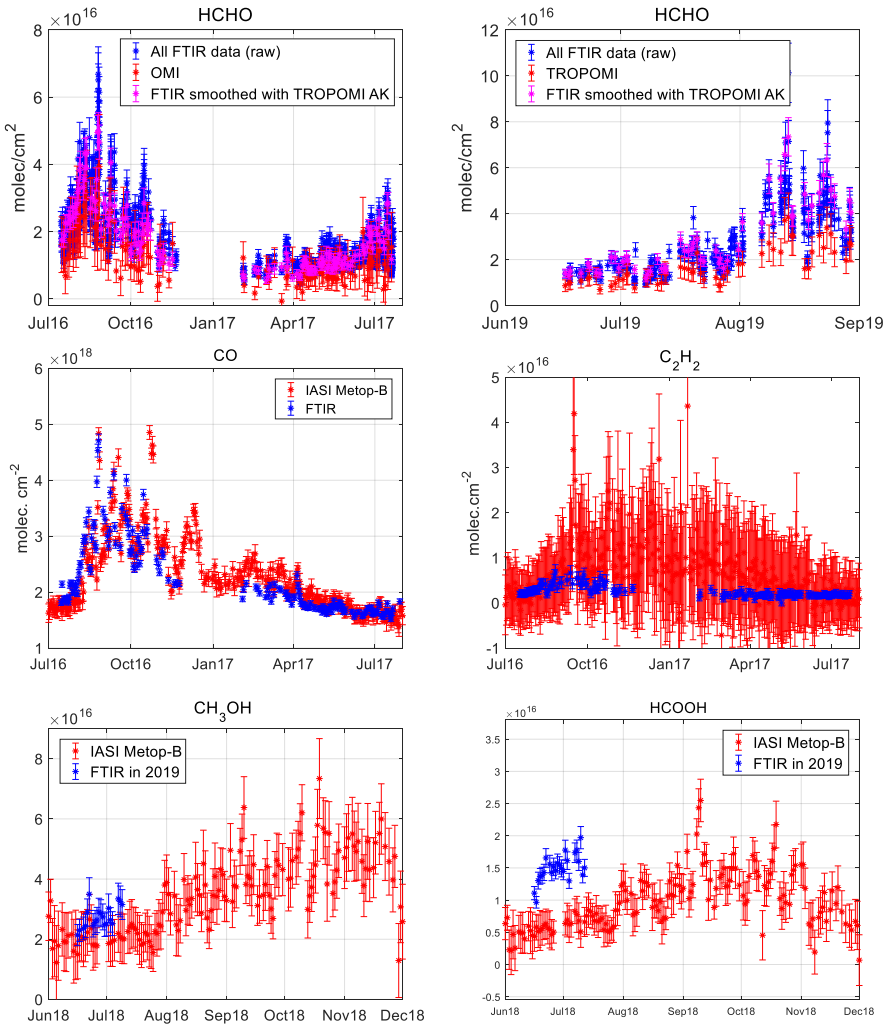

Figure 11: Top panel: FTIR and satellite data in case of HCHO (OMI and TROPOMI); middle panel: CO and C_2H_2 (IASI; Metop-B) for the July 2016-July 2017 period; bottom panel: CH_3OH and HCOOH from IASI Metop-B in **2018** compared to our June-July **2019** data. The error bars correspond to the total error (random and systematic),

to check if the compared instruments agree within their total error bars. For OMI and TROPOMI, the data are averaged within 150 and 20 km around the station, respectively, and within 6 hours. For IASI data, daily means are used, within 200km around the station.

The statistical comparisons with satellite data are summarized in Table 2. We provide the mean of the differences ("Bias"), mean(SAT-FTIR)/mean(FTIR), and the 1-σ standard deviation (STD) of the differences, std(SAT-FTIR)/mean(FTIR). The bias and STD can be compared to the combined (SAT and FTIR) systematic and random error budget when available. We also provide the Pearson correlation coefficient.

For the OMI and TROPOMI validation, we use the Rodgers and Connor (2003) formalism for the validation, because the satellite files provide total column averaging kernels and a priori profile information; therefore the validation can be made taking into account the low vertical resolution of the instruments. A negative bias of -28% is observed in OMI data, but it is well within the systematic error budget of the differences (45%). A similar bias (-37%) is observed in the recent TROPOMI satellite, which is expected due to the similar algorithm developed for both satellite products. Within other projects funded by Beslpo (TROVA and TROVA-2), we have performed the HCHO TROPOMI validation using more than 20 FTIR stations. The mean bias at all stations was -15%, with the largest negative biases (-24 to -46%) observed at polluted sites (Paris, Xianghe, Mexico City). Our Porto Velho site confirms the negative bias of TROPOMI when high levels of HCHO are observed. The correlation coefficient is very good between OMI and FTIR (0.80), and indeed both instruments observe very well the seasonal variability of HCHO (Fig.11). The STD of the differences is however larger (31%) than the combined random error budget (7%). A similar result is obtained in TROVA-2 with the TROPOMI validation at polluted sites: the collocation error is obviously larger at higher polluted areas, and the random error of OMI / TROPOMI might be underestimated, or partly systematic. The collocation has been chosen to be within 6 hours and 20 km. Stricter collocation choices have been tested but do not improve the comparisons due to larger satellite random errors when the number of averaged pixels decreases.

Table 2: Statistical mean differences ("bias") and standard deviations (STD), between collocated SATELLITE (SAT) and FTIR data. The systematic and random uncertainties on the differences are also given, as well as **the correlation coefficient between the two data sets.**

SAT product	Bias ± STD SAT – FTIR / mean(FTIR)	Combined Systematic Error	Combined Random Error	Correlation R
OMI HCHO	-28 ± 31 %	45%	7%	0.80
TROPOMI HCHO	-37 ± 20 %	27%	11%	0.62
IASI CO	-0.5 ± 13.7 %	6%*	6%*	0.90
IASI C_2H_2	+98 ± 146 %	390%*	390%*	0.40

* At present, IASI provides only one uncertainty which is a combination of random and systematic. We then have chosen to use them for both columns in this Table and without dividing them by sqrt(nb collocation). Therefore, these uncertainties can be seen as upper limit, and are probably overestimated.

IASI CO validation:

The IASI CO product has been developed by the LATMOS-IPSL, in collaboration with ULB (George et al., 2015). The agreement between IASI and FTIR is very good: a very small bias (-0.5%), and a very good correlation coefficient (0.90). However, it looks from Fig. 11 that IASIhas a negative bias during the dry season (July-September; -8.5%) and a positive one during the rest of the year (October-May; +5.5%), but more years are needed to check if this is a systematic effect occurring each year. The standard deviation is larger than the combined random uncertainties, but this is likely due to the collocation effect when the variability is high: indeed the standard deviation is only 6.7% during the Oct-May period (with a correlation coefficient of 0.96), while it is 16.3% during the biomass burning activity period (with a still very good correlation coefficient of 0.90).

IASI C_2H_2 validation:

FTIR data from 2 stations have been used in the past for the C_2H_2 IASI validation (Duflot et al., 2015), and showed contrasting results: IASI was 107% higher at Reunion Island, and 12% lower at Jungfraujoch. The new C_2H_2 IASI data set used in this report has been developed by B. Franco (ULB), in the framework of the OCTAVE project (Belspo), and has not been published yet. It is based on a neural network approach, which is also applied to the IASI CH_3OH and HCOOH data shown in Fig. 11, and published recently in Franco et al. (2018). **IASI is largely higher than FTIR (+98%)**, but this bias is not constant over the year: we obtain a reduced bias of +35% during the April-July period.

This IASI data set is still under development and this validation result shows that more investigation is required in order to understand the high bias at Porto Velho.

IASI CH_3OH and HCOOH validation:

We cannot quantitatively compare IASI and FTIR data yet, because we only have CH_3OH and HCOOH FTIR data for June-July 2019, while the IASI data sets only reach up 2018 at present. However, looking at Fig. 11, where the IASI data in 2018 has been plotted together with the 2019 FTIR data (only June-July, before the August intense fires in 2019), we can see **that IASI is biased low for both species, but much more for HCOOH (-58%) than for CH_3OH (27%).**

CH_3OH and HCOOH IASI comparisons will also be performed at the Reunion Island site within the OCTAVE project, and we will be able to see if the satellite performs in the same way at two sites with different VOCs levels (Reunion is a remote site in Indian Ocean), but using the same harmonized retrieval settings.

2.4. WP4: Comparison with IMAGES model

We compare, in Fig. 12, our FTIR time-series (HCHO, CO, C_2H_6, and C_2H_2) with the IMAGES model developed at BIRA (J.-F. Müller, T. Stavrakou, M. Bauwens, see e.g.Bauwens et al., 2016). Model data for 2019 are not available yet, therefore we do not compare CH_3OH and HCOOH species. IMAGES does not provide HCN.

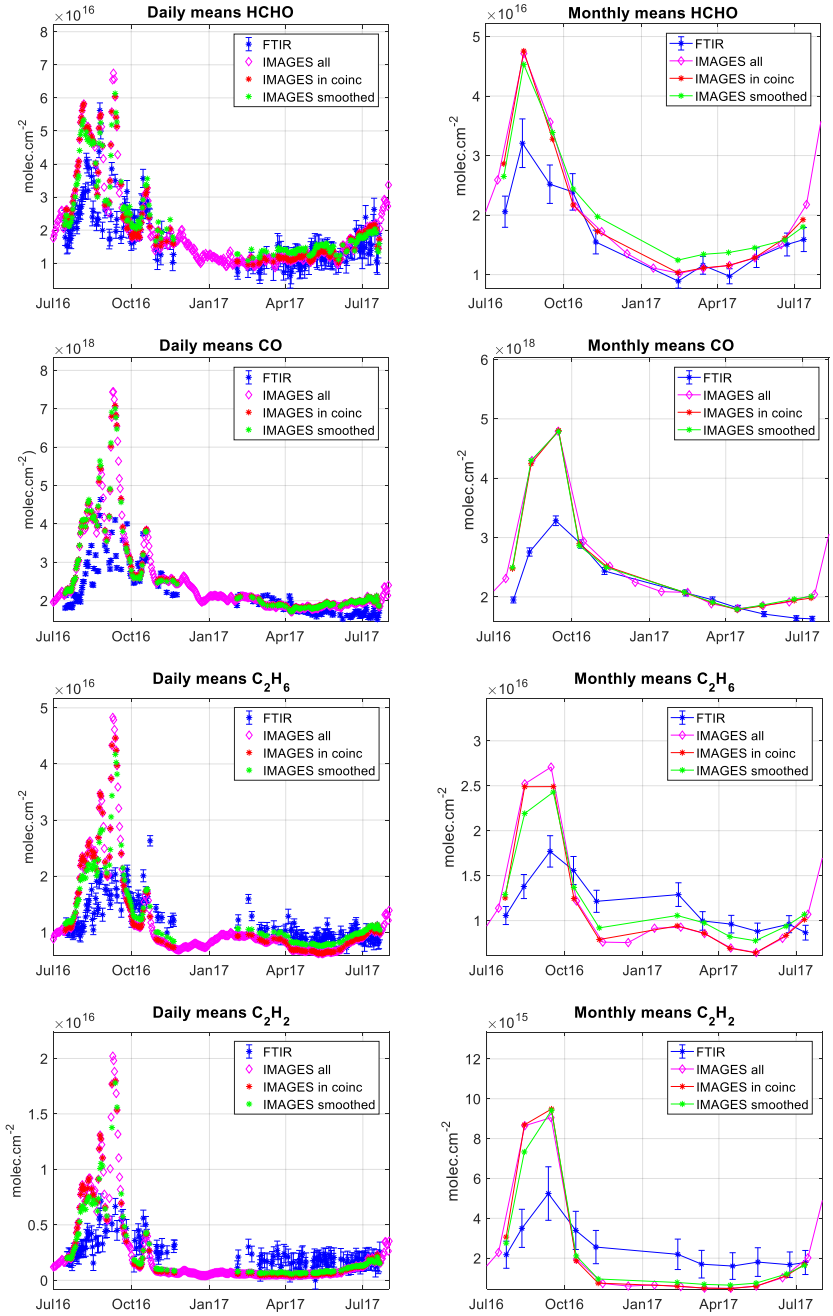

Figure 12: Daily (left) and monthly (right) means of HCHO, CO, C_2H_6, and C_2H_2 total columns at Porto Velho from FTIR measurements (blue) and IMAGES model. The magenta diamonds are all model data, while the red stars are IMAGES data in daily coincidence with FTIR. The green stars are the model total columns when the modelled profiles have been smoothed by the FTIR averaging kernels (AK), following the Rodgers formalism (Rodgers and Connor, 2003).

We give in Table 3 the statistical comparisons of the daily means differences, for 2 different time periods: the dry season (July-September), and the rest of the year (October-June).

Table 3: Statistical bias and standard deviations (STD), between daily means of model and FTIR data.

	Bias ± STD IMAGES-FTIR/mean(FTIR) **July - October**	**Bias ± STD** IMAGES-FTIR/mean(FTIR) **November - June**	**Correlation** Daily means All year	**Correlation** Monthly means All year
HCHO	+ 27 ± 36 %	+ 20 ± 20 %	0.83	0.96
CO	+ 32 ± 35 %	+ 7 ± 9 %	0.82	0.88
C_2H_6	+ 26 ± 42 %	- 11 ± 13 %	0.69	0.80
C_2H_2	+ 42 ± 89 %	- 62 ± 33 %	0.74	0.89

HCHO model comparison:

Formaldehyde is the species for which we find the best correlation between the model and the FTIR data (0.83 for the daily means, and 0.96 for the monthly means, which is also seen in Fig.12 with a very good agreement between the seasonal cycles). Formaldehyde is the only species for which the bias is of the same order (in %) during the two seasons (Table 3). This would suggest that the emissions that are overestimated could be related to other emissions than the biomass burning database. We can however note that in absolute terms the overestimation is still more important during the dry season (6.6E15 compared to 2.5E15 molec/cm^2), so biomass burning could be an additional effect, and seems to be confirmed with the overestimation of all our other biomass burning species in the dry season.

Our HCHO results are currently used in a study conducted by our IMAGES model colleagues: they make an inversion of 13 years of OMI HCHO data to obtain a top-down VOC emission estimates over South America, using a new version of IMAGES, called MAGRITTE, with a better horizontal resolution (0.5°x0.5°, instead of 2°x2.5°). This work has been presented at the EGU 2019 conference (M. Bauwens, poster presentation), and will be published soon. Their main finding is that the model a priori (before inversion of OMI) was largely overestimating HCHO over South America compared to OMI data. This is in agreement with the 27% and 20% overestimation of IMAGES data compared to our FTIR measurements at Porto Velho. The inversion of OMI data leads to significant emission decreases: -39% for isoprene (the main HCHO precursor) and -21% for fire fluxes in the whole South America region, and to even -50% for isoprene in the tropical rainforest region. This work is validated against FTIR measurements at our site, and at Paramaribo (Surinam), the only other FTIR site in South America, operated by the University of Bremen. We provide in Fig.13 the comparison of MAGRITTE and OMI (left panel) and MAGRITTE and FTIR (right panel), as shown in the EGU 2019 conference. We see that, although the sites are very different (Paramaribo has a much weaker seasonal cycle), the bias between the model a priori and the satellite is very similar (about +38-39%) at both sites, as well as the bias between the model a priori and FTIR (about +22-27%) at both sites. We see that the optimized model

(after inversion of OMI data) show more decrease at Porto Velho (near the rainforest), than at the more coastal site Paramaribo. **The inversion brings the model closer to the OMI data at Porto Velho (bias reduced to -3%), but it also brings the model to too low values compared to our FTIR measurements (-19%). This is in agreement with the negative bias observed between OMI and FTIR data (Table 2).**

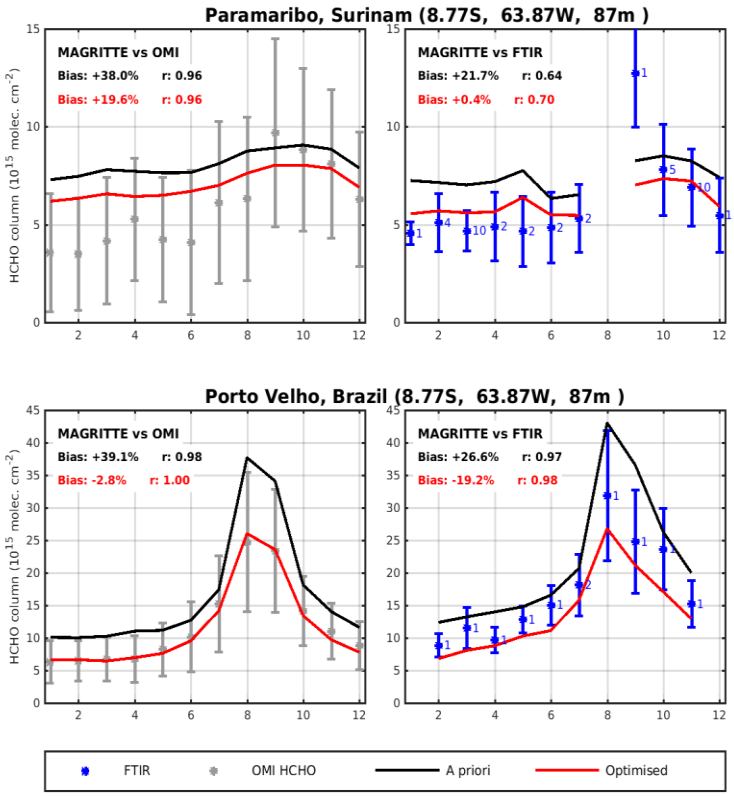

Figure 13: MAGRITTE model and OMI HCHO (left panels) and MAGRITTE model and FTIR HCHO (right panels) at Paramaribo (upper panels) and Porto Velho (lower panels).

At present, we performed OMI and FTIR comparisons only at Porto Velho, but this will be done (I. De Smedt) using the network of more than 20 stations measuring HCHO with harmonized retrieval settings that was built in our project TROVA. If we find, as we did during the TROPOMI validation (TROVA-2) than the OMI satellite is underestimating HCHO at all polluted sites (not only Porto Velho), **this should lead us to question the inversion results and/or its methodology: could the satellite known negative bias be corrected prior to its inversion by models ? This would avoid to have underestimated emissions in the model.**

CO model comparison:

We find a good correlation between the model and the FTIR data (0.82 for the daily means, and 0.88 for the monthly means). The comparison with the model is good for CO during the November-June period, with a small bias of +7% (higher for the model). However, the bias is much larger during the biomass burning season (+32%). This overestimation of the model during the biomass burning season is observed in all the species. This points to a **likely overestimation of the burned material in the fire emission database used in the model (GFED4) during the August-September 2016 months, and/or to too large emission factors of all the species in the model.**

C_2H_6 model comparison:

As discussed previously, the model overestimates all species during the biomass burning period (+26% for C_2H_6). This is a bit lower than for CO, but on the other hand, the model underestimates C_2H_6 during the Nov-June period (-11%), pointing to another source that should be underestimated. This source might be anthropogenic because the anthropogenic emissions are roughly constant over the year. Therefore, increasing the anthropogenic emissions would reduce the Nov-June negative bias of the model, while increase the positive bias during the biomass burning period to some values closer to the CO bias (+32%). **Our comparison suggests that the anthropogenic emission database used in the model (EDGARv.4.3.2), might be about 10% too low for C_2H_6 over South America.**

C_2H_2 model comparison:

The correlation between the monthly means of the model and FTIR C_2H_2 data is very good (0.89). However, a large underestimation of the model is observed in in November-June (62%). This is due to the fact the biofuel emissions, important in Brazil, are not reported in the anthropogenic emission database EDGARv.4.3.2 used in IMAGES (T. Stavrakou, personal communication). Even with this large underestimation of anthropogenic emissions, the model still overestimates C_2H_2 during the biomass burning season (+42%).

Enhancement ratios: comparison with model

To check if the overestimation of the model observed for all the biomass burning species is due to an overestimation of the burned material in the fire emission database used in the model (GFED4), and/or to too large emission factors in the model, we compare here the enhancement ratios obtained from our FTIR data to the ones calculated from the emission factors used in the model.

Similarly to what was done in Vigouroux et al. (2012), we can use our correlation plots of our species (X = C_2H_6, HCN and C_2H_2) with CO (Fig. 7) to obtain their enhancement ratios ER = ΔX/ΔCO, and compare this to the literature. Indeed, if we assume that the excess total columns of X and CO are due to the biomass burning events, following Hornbrook et al.(2011), these slopes represent the "normalized excess mixing ratios" (also called the "enhancement ratios" as the plumes are far from the emission sources, as opposed to the emission ratios at the source, as defined in Andreae and Merlet,(2001). Following Andreae (2019), we derive the model and the literature enhancement ratios (ER) from the equation:

$ER = EF_X / EF_{CO} * MW_{CO} / MW_X$, (Eq. 1)

where MW_X and MW_{CO} are the molecular weights of the species X and the reference species CO, and EF_X and EF_{CO} are the emission factors used in the model and provided usually in the literature, for the species X and for the reference gas CO.

We give in Table 4 the enhancement ratios determined by the slope ΔX/ΔCO obtained from our measurements (Fig. 7). As our Flexpart simulations show that most of our FTIR data are coming from the tropical forest vegetation (see WP5), we compare our enhancement ratios to the values used in the model (after conversion using Eq. 1) for tropical forest, and given in the most recent publication on emissions factors (Andreae, 2019) for tropical forest, based on compilation of many field measurements.

Table 4: Enhancement ratios derived from FTIR measurements at Porto Velho, compared to the model and the Andreae (2019) compilation.

X	Our FTIR data	Model IMAGES Tropical forest	Andreae (2019) Tropical forest
HCHO	0.011	0.0224	0.0215
C_2H_6	0.0047	0.0088	0.0079
HCN	0.0030	-	0.0044
C_2H_2	0.0017	0.0046	0.0036
HCOOH	0.013	0.0060	0.0029
CH_3OH	0.021	0.026	0.022

We see in Table 4 that the enhancement ratios used in the model for tropical forest, are about a factor 2 larger for HCHO and C_2H_6, and even almost a factor 3 for C_2H_2. This could explain the overestimation of the model for all these species, especially the fact that the model is still too large for C_2H_2 in the biomass burning season while the anthropogenic emissions are so much underestimated.

The model emission factors are coming from the literature (Andreae and Merlet, 2001; and various updates), and we see in Table 4 that the latest publication (Andreae 2019) shows also larger values than our FTIR measurements (except for HCOOH and CH_3OH). However, the uncertainties on the emission factors given in the literature are quite large (from 25% for HCHO to more than 100% for C_2H_2). Therefore, it is not an easy task for modellers to choose a value.

In the coming months, when our FTIR data will covered another biomass burning season in 2019, and when we will have model data for the 2019 year as well, sensitivity model studies will be made using our FTIR enhancement ratios instead of the current ones. It was planned to make sensitivity studies during IKARE, but the fact that only one year of data was available (Task 1.1) makes it hard to conclude definitely if the overestimation of HCHO, CO, C_2H_6 and C_2H_2 is due only to the too large emissions factors or also to an overestimation of the burned area**. More years can decoupled the 2 effects.**

At the time of this report, we do not have IMAGES data for 2019, therefore comparisons with HCOOH and CH_3OH are not possible. However, we already see that the FTIR enhancement ratio for CH_3OH (0.021) is similar than the one used in the model (0.026), and agrees well with the one provided in Andreae et al. (2019). On the opposite, the obtained FTIR enhancement ratio for HCOOH (0.013) is much larger than the one used in the model (0.006), and the one provided in the recent paper (0.0029). This too low emission ratio used in the model for biomass burning sources can, at least partly, explained the very well-known underestimation of HCOOH in the current models (Stavrakou et al., 2012; Paulot et al., 2011).

2.5 WP5: Explore the impact of different vegetation sources on the FTIR data

Flexpart (Stohl et al., 2005) is a Lagrangian transport model which effectively tracks an array (in our case 200000) of individual particles as they make their way through the atmosphere from a release point (forward trajectory) or towards an observation point (backward trajectory). The model itself is driven by global 1°x1°- 137 vertical levels - operational wind fields from ECMWF. Its major advantage over classic Eulerian models is that it provides a direct link between source areas and observation point, nor does it suffer from artefacts induced by the gridding process of said models. However, due to the individual nature of each tracked tracer particle, no advanced chemistry is feasible within the model. Flexpart only takes into account a first order decay rate due to the reaction of the species of interest with OH (taken from the GEOS-CHEM model, Bey et al., 2001). Given that this is, for most species, the dominant removal pathway, it yields good results. However, particularly for species that have more complex formation/destruction pathways (for instance, formaldehyde is predominantly formed from various emitted precursor VOCs), Flexpart cannot be used. **Given the above limitations and our focus on the South-American continent we opted to initiate our study, based on our C_2H_2 measurements as its atmospheric lifetime of several days limits contributions from other continents while at the same time is sufficiently large for emissions throughout the continent to reach our measurement site in Porto Velho.**

To study the predominant source regions we have run back-trajectories for each individual FTIR measurement. We then paid particular attention to the so-called footprint layer (between the surface and 250m) where emissions enter the atmospheric boundary layer and commence their transport. Our analysis shows that, by far, **the dominant source regions are located over the Amazon rain forest stemming from air masses coming in from the East (see Fig. 14).** During the local summer months, we see a more Northern angle of the Eastern

approach while otherwise a more Southern pathway becomes dominant (Fig. 14). In some instances, the footprint covers sections of Western Africa. Of the 835 measurements analysed, 178 (~20%) also show contribution from a second pathway coming from the South (see Fig. 14-bottom left). However, it is rare for this pathway to become dominant.

Both observations (the predominant eastern airflow and the seasonal variability thereof) are linked to the influence of the Inter Tropical Convergence Zone (ITCZ) where Northern and Southern tropical winds converge. The location of this zone follows the thermal equator (located along the longitudinal band where mean temperatures reach their highest point), which in turn is influenced by the position of the solar equator. The latter is located South of Porto Velho from end October until end February. This causes the ITCZ to shift southwards during local summer, exposing Porto Velho to wind directions coming from the North-East.

For the purpose of binning the measurements in different transport scenario cases (see further), we distinguish 3 categories. NE (distinct North-Eastern approach), SE (distinct South-Eastern approach) and S (distinct Southern approach), examples of each being shown in Fig. 14. Of course in several cases, no clear distinction could be made between the different scenarios (when ITCZ is mid-shift or when a minor contribution from a Southern pathway is present).

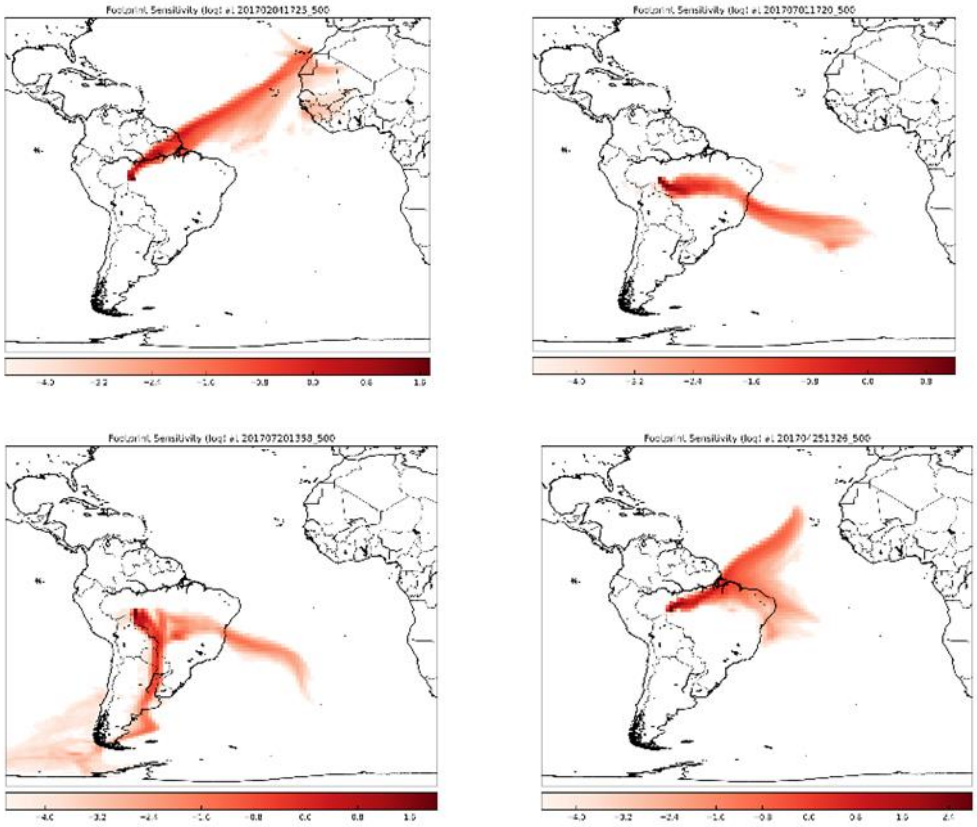

Figure 14: Examples of 3 distinguished pathways: North-East (top-left), South-East (top-right), South (bottom-left), and an example of a pathway that could not be easily categorized (bottom-left).

Unfortunately, these rather steady airflow patterns do not yield great variability in source region composition. To quantify the contribution of different vegetation types on the observed signal we have folded the Flexpart derived residence times near the surface (<250m) with the allocated vegetation type. Here we used the map (see Fig. 15) from Stone et al. (1994), derived from the NOAA Advanced Very High Resolution Radiometer (AVHRR). This high resolution (1km^2) map was first binned into a courser 0.5 x0.5° Flexpart output resolution grid without negating the vegetation composition within said grid. **The most predominant category was "Tropical moist and semi-deciduous forest"** (referred to as "moist Tropical forest" throughout this document for brevity). Typically, the fraction of time spent in the footprint area above this vegetation type ranges around 70% with some rare offshoots to 90 and 40% (see Fig. 16). Two other vegetation types that often play a role are "Cleared Tropical Forest", "Seasonal woodlands" and "Savanna/grasslands". Two example pie charts with fractional contributions from different vegetation types are given in Fig. 17.

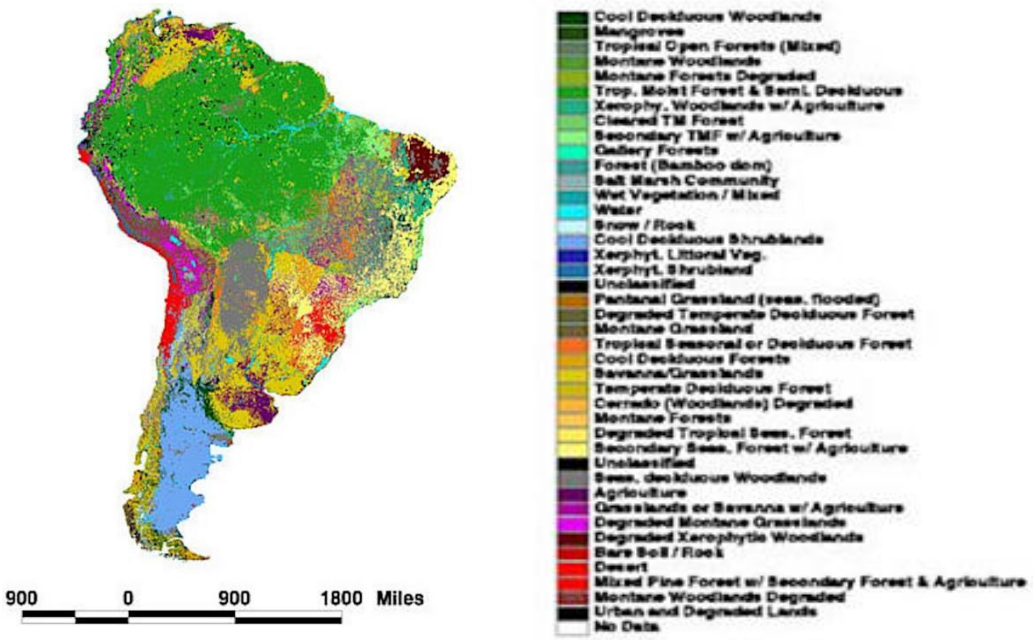

Figure 15: NOAA Advanced Very High Resolution Radiometer (AVHRR) derived vegetation map for South-America.

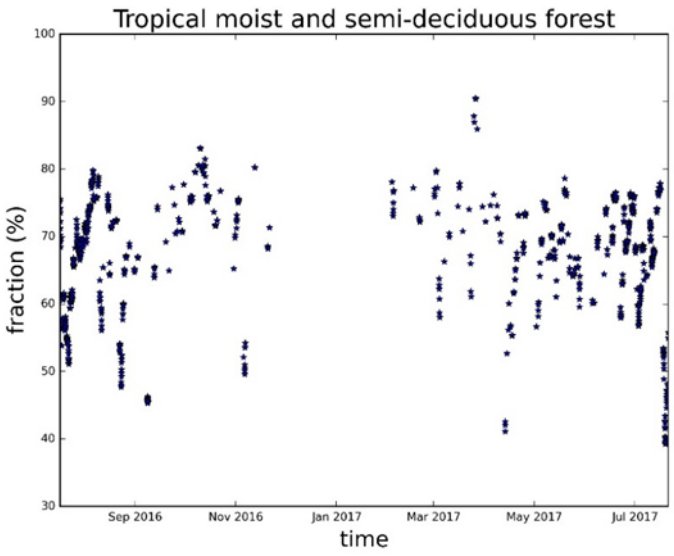

Figure 16: Time series of the fraction of near surface residence time spent in the boundary layer above moist Tropical forest.

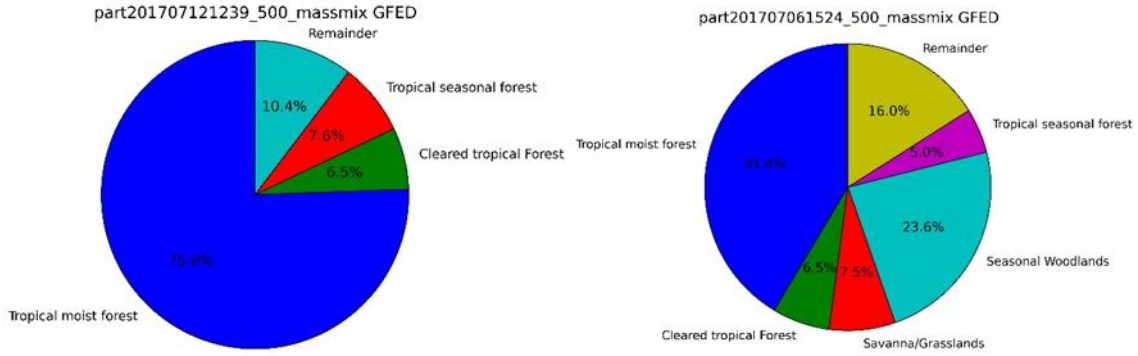

Figure 17: Examples of the fractional breakdown of near surface residence times above different vegetation types

Flexpart-GFED analysis

The air mass-folded near-surface residence times generated by Flexpart (s m^3 kg^{-1}) can be multiplied by the estimated emissions (kg m^{-2} s^{-1}) fluxes to generate a mass mixing ratio (with respect to air) as observed at the FTIR site, which is then converted to a dry air mole fraction using the 28.96/26.04 ratio. This study took into account basic fire emission height suggestions by Dentener et al. (2006) although for future analysis we will look into Sofiev et al (2012), which paints a far more realistic picture. These simulated concentrations can then be compared with our actual measurements. We performed Flexpart simulations for different altitude brackets, one of which represented air arriving at Porto Velho near the surface (between 0 and 500m) and one that corresponds with a column between 0 and 10 km). These have been compared with the corresponding FTIR measurements. The emissions in question were taken from the GFEDv4.1s fire emission database. Note that for 2017, GFED

currently only provides a beta version, which extrapolates fire count data directly into burned mass estimates based on previous years' analysis. We do not, at this point, take a look at other emission sources such as bio-fuel consumption as we want to focus our attention on the enhancements seen during the biomass burning season.

To calculate the source region associated with the Flexpart-GFED emissions, we again coupled the outcome to the NOAA Advanced Very High Resolution Radiometer (AVHRR) derived vegetation map (as seen above), calculating the relative composition of the emitting source areas on the simulated total. **Again the dominant source region is moist Tropical forest, which we show in Fig. 18, but with a stronger variability, where in the biomass burning season the contribution consistently hovers around 70%, outside the fire season the relative contribution shows very high variability and drops to values as low as 0%.** Note that the simulated Flexpart-GFED concentrations are very low in this January 2017-June 2017 timeframe. If we focus on 2016 alone we see a drop in relative contribution from ~70 to ~30% after mid-September. This coincides with an almost complete disappearance of the simulated fire emission spikes. To study this particular aspect, we have binned the dataset into a group consisting of data points with a less than 50% Tropical rain forest emission contribution and a group with more than 70% contribution (see further below).

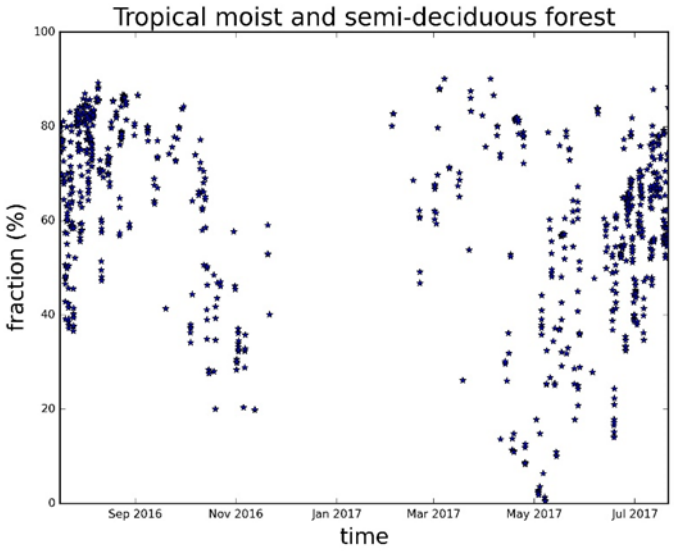

Figure 18: Time series of the fraction of Flexpart-GFED moist Tropical forest contribution.

Figures 19a and 19b show time series of FTIR (red) and Flexpart-GFED simulated (blue) C_2H_2 concentrations for the 0-500m (Fig. 19a) and 0-10 km partial column average volume mixing ratios (Fig. 19b). It is immediately clear that for the near surface data, the Flexpart simulated concentrations exceed those of FTIR, while for the 0-10 km layer the opposite is true. This is not surprising. The vertical resolution of FTIR profiles is very limited and therefore the near-surface values, obtained by the FTIR instrument, are heavily influenced by concentrations in the mid-and even upper troposphere and is thus far less responsive to changes near the surface. In addition, the C_2H_2 emission ratio used in the Flexpart-GFED simulations is in line with the IMAGES model one (Table 4), which has been found to be much larger than the one coming from our FTIR data (see WP4). For the 0-10km simulation, Flexpart will hardly pick

up any source footprint for the upper troposphere, as the simulation is limited to 10 days, which limits transport from the surface to higher altitudes. This makes a straightforward quantitative analysis difficult. Also apparent is a strong increase in simulated Flexpart C_2H_2 concentrations from July 2017 onwards. This increase is absent in the FTIR data. While the trajectories from the 17th of July 2017 consistently show a strong contribution from Southern source regions (and thus a stronger contribution of savanna fires), the simulated increase covers the entire July period and **points to a problem with the provisional emission fields in the 2017 GFED beta release.**

Also visible are some very strong outliers in the simulated Flexpart-GFED analysis, particularly up to and including September 2016. The total emissions calculated are in part due to the Flexpart analysis, the course fire injection heights used, the GFED estimation of total biomass burned and the emission factor for that particular species and vegetation. When we see a constant offset, meaningful conclusions on these emission factors can be drawn but in this case, an overestimation of the total burned biomass within GFED 4.1s within this period looks to be in play as other factors would likewise impact 2016 data as well.

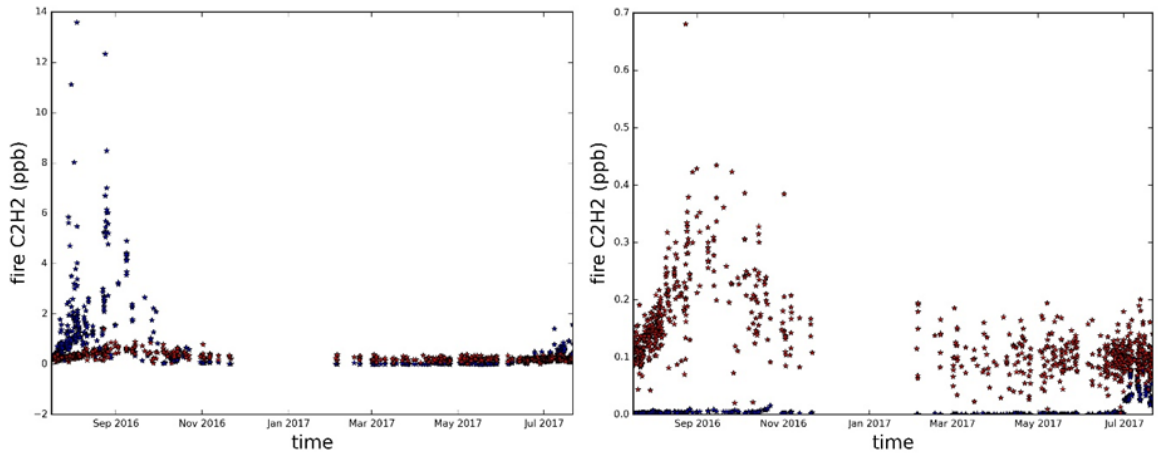

Figures 19a(left) & 19b(right): Time series of FTIR (red) and Flexpart simulated (blue) C_2H_2 concentrations, near the surface (left) and between 0 and 10 km (right).

We also plotted the correlations between both datasets, limited to the year 2016. These are shown in Fig. 20. For the lowest layer we obtain a correlation coefficient of 0.40 while for the tropospheric column we obtain a coefficient of 0.62. These are moderate values but again we need to take into account the difference in vertical sensitivity. The intercept of the 0-500m analysis is near zero, indicating that for this layer all variability is primarily due to biomass burning (given that we only simulated GFED emissions). For the 0-10km analysis we do see an intercept, but it is the inverse of what we would expect if there was a significant non-biomass burning contribution. Therefore, we can safely conclude that biomass burning plays a dominant role in the time series analysed. An important caveat here is that, due to the issues suspected in the preliminary 2017 GFED dataset, we limited our analysis to the 2016 dataset, which in itself does not cover the entire year and is restricted to the biomass burning season. If we take the entire time series, looking at the intermediate January till May 2017 period we see that in both cases (0-500m and 0-10km) the simulated concentrations are

lower than the FTIR measurements, both of which with little seasonal variability and magnitude.

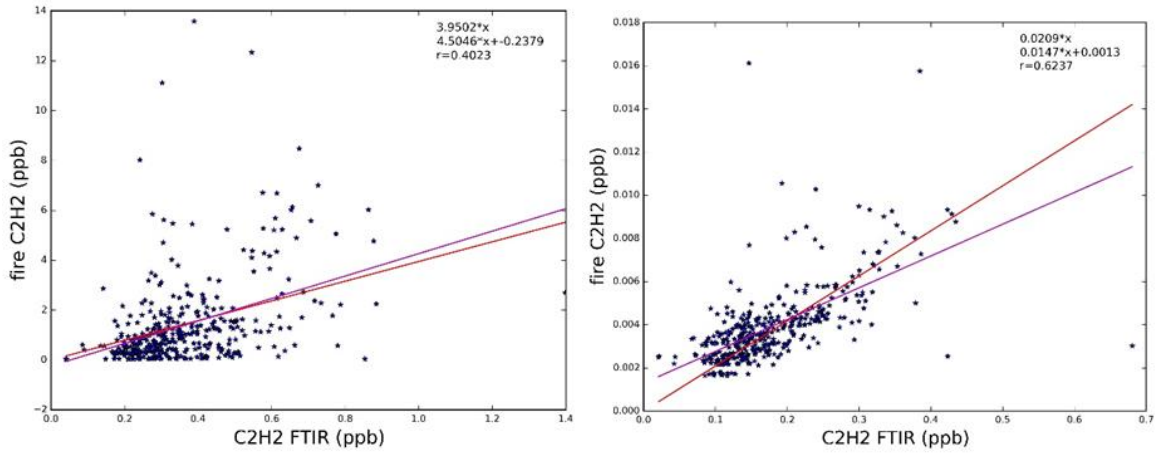

Figure 20: Correlation plots between FTIR and Flexpart simulated C_2H_2 concentrations, near the surface (left) and between 0 and 10 km (right). The red line corresponds with a slope forced through 0, while the magenta line corresponds with a standard linear fit.

As mentioned above we also looked at differences within the dataset based on the trajectory pathway (see Fig. 14 and the discussion thereof). For the 2016 dataset, only the Southern and South-Eastern pathway appeared in sufficient numbers. The correlation plots of both these data subsets are shown below in Fig. 21. Only for the South-Eastern, 0-500m simulation (bottom-left) do we see a strong decrease of the correlation coefficient (note that for the 0-10km simulations these are not affected in this sense). Slopes differ between the pathway datasets but given the number of substantial outliers (who have a significant effect upon the limited dataset) it is too early to claim any significant difference due to the GFED employed emission factors. The upcoming update of the GFED 2017 database, and the release of a 2019 (hopefully good) beta version, would allow us to include 2017 data with confidence and expand our analysis dataset into 2019.

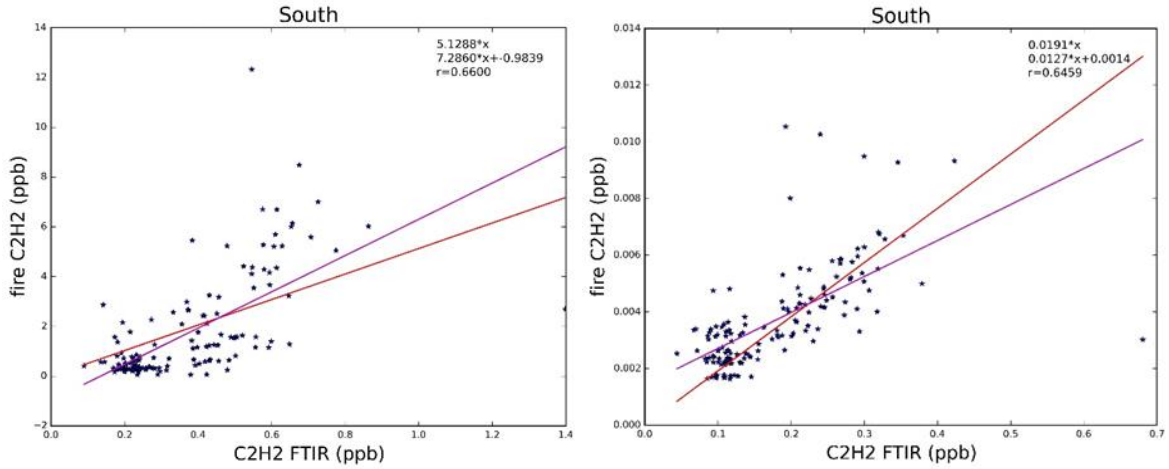

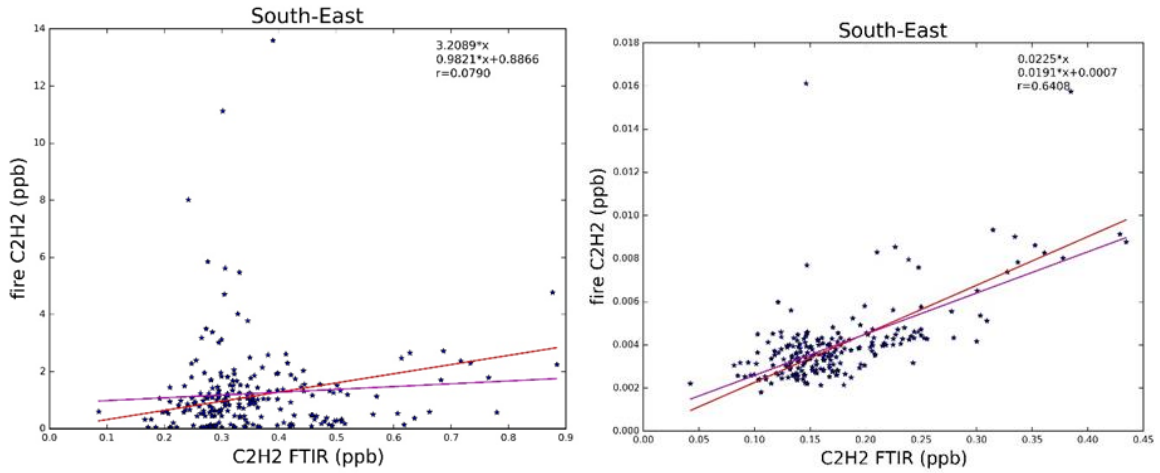

Figure 21: Correlation plots for Flexpart simulations with a substantial Southern (top) and South-Eastern (bottom) pathway for 0-500m (left) and 0-10km (right).

We also binned the data in 2 groups based on the relative contribution of Flexpart-GFED simulated moist Tropical forests' emission contribution to the total signal (we also performed a binning based on the raw residence times without the inclusion of GFED which yielded similar results). The results are shown in Figs. 22 and 23. The $<50\%$ time series represent far lower concentrations than the $>70\%$ group, which is expected given the predominant source of biomass burning emissions. In fact for the $<50\%$ group the simulated Flexpart-GFED emissions are of the same order of magnitude as the measured FTIR values for the 0-500m analysis. For the $>70\%$ group, the simulated values far exceed the FTIR measurements, including the already mentioned spikes in the time series. High (>0.6 ppb) FTIR values can be seen in both groups. Given the lower concentrations (and variability) and fewer data points the correlation for the $<50\%$ group is lower than the $>70\%$ group. For the 0-10km analysis, the order of magnitude of the Flexpart-GFED simulated data is the same for both groups. Note that the chosen cut-off has been taken rather arbitrarily to ensure enough data points yet still have a separation. Nor can we really regard $<50\%$ as a low contribution, furthermore we also see strong peaks in the intermediate 50 to 70% range.

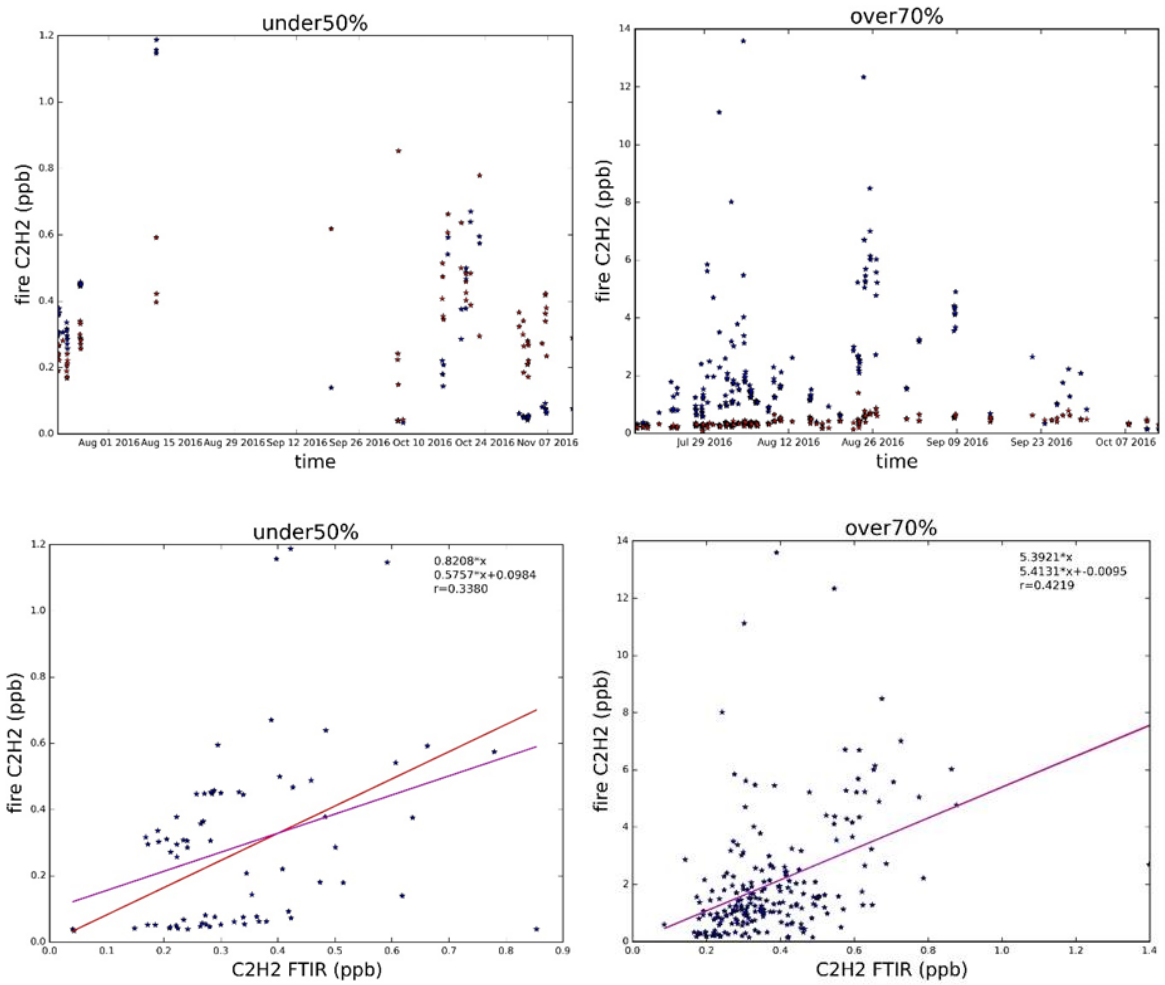

Figure 22: 0-500m time series (top) and correlation (bottom) plots between FTIR and Flexpart simulated C_2H_2 concentrations, for a subsection of data based on the relative Flexpart-GFED emission contribution over Tropical moist and semi-deciduous forests. On the left less than 50%, on the right more than 70%.

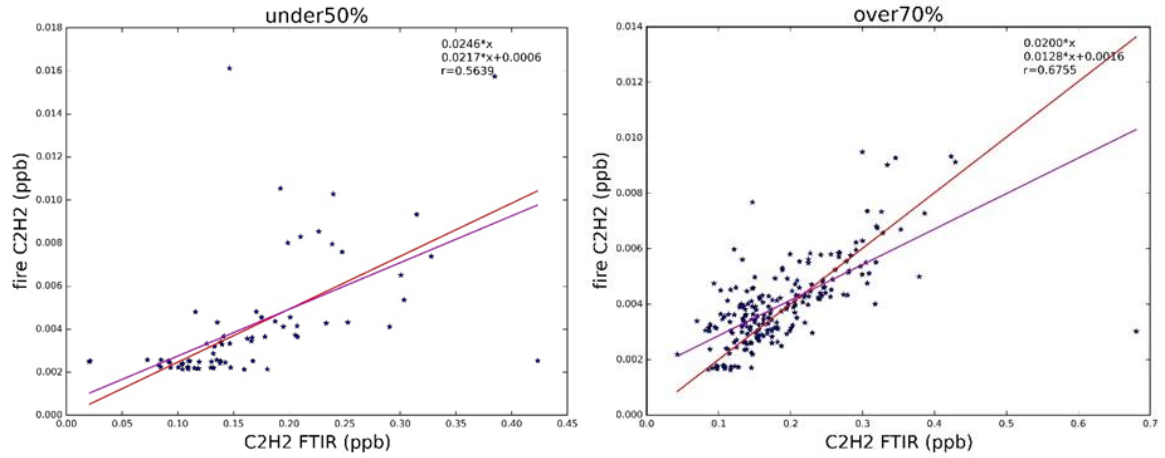

Figure 23: 0-10km Correlation plots between FTIR and Flexpart simulated C_2H_2 concentrations, for a subsection of data based on the relative Flexpart-GFED emission contribution over Tropical moist and semi-deciduous forests. On the left less than 50%, on the right more than 70%.

Regardless of the data subset used, strong mismatches between Flexpart-GFED and our observations are ever present. Given the random nature of the simulated uncorrelated peaks, this is not so much a problem of the GFED employed emission factors but rather points to either a failure of Flexpart to accurately capture the emissions and transport thereof or the estimated burned matter (from which the C_2H_2 concentrations are derived using a fixed emission factor) with GFED 4.1s over tropical forest areas. Flexpart could potentially be improved by using higher resolution ECMWF wind fields and better parameterization (with regards to its emission injection heights) but it remains to be seen though, given the rather uniform transport pathways, if this is the critical component rather than GFED. For instance, intense fires contain a significant amount of latent heat, which impacts the vertical convection scheme of Flexpart. **To draw conclusions on the emission factors employed by GFED, the inclusion of 2019 data would certainly go a long way, as at this point the partially captured 2016 fire season yields too little data to confidently smooth out the variability within.**

Enhancement ratios related to different vegetation type

One of the objectives of this WP5 was also to use the distinction between the different vegetation giving a high contribution to the FTIR observations to calculate different enhancement ratios in function of the type of burned vegetation. However, this turns out to be difficult since only one main vegetation has been identified to give large contribution at present (Tropical moist and semi-deciduous forest, see Figs. 17 and 18). We do not have enough FTIR data coming from e.g. >70% savannah, to derive associated emission ratios.

When more years will become available, we might be able to measure fires from the savannah (if winds allow). Then the filtering can be made on FTIR data to obtain corresponding enhancement ratios. We give an example of what can be done in Fig. 24, with the Tropical moist and semi-deciduous **forest contribution highlighted in the FTIR data.** No clear distinction, for this single year of data, is seen in the correlation plot with CO between the data with more than 70% contribution coming from the Tropical and semi-deciduous forest, which is the reason why we have used all the data up to now to derived our enhancement ration in WP4. Once clear data can be extracted coming from e.g savannah, we will do so.

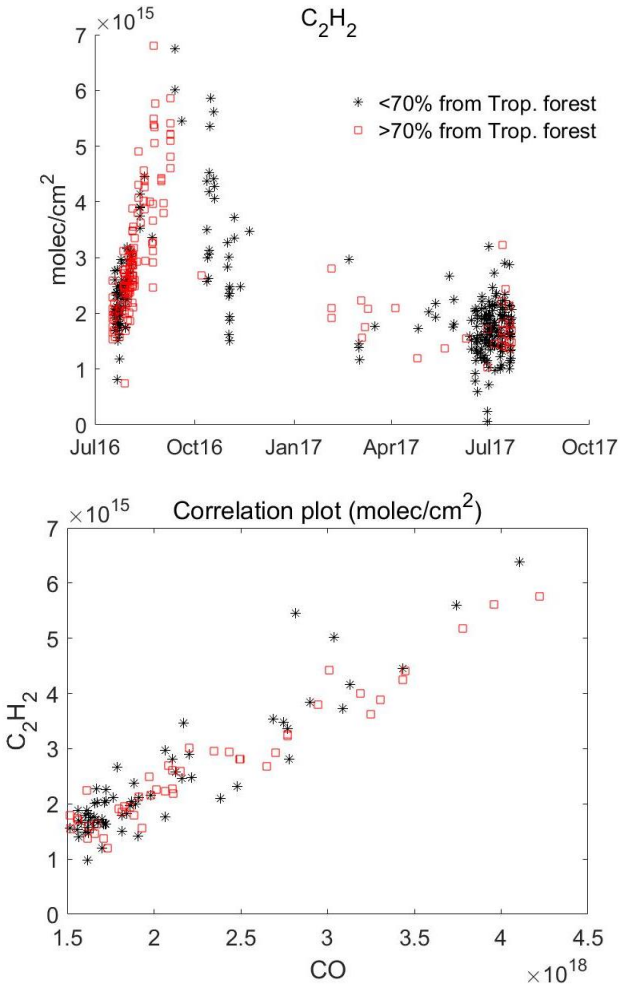

Figure 24: Filtering of FTIR data using the Flexpart-vegetation map combination: here in red the FTIR data identified to be for >70% coming from Tropical moist and semi-deciduous forest. Left: 2016-2017 C_2H_2 total columns time-series. Right: correlation plot with CO.

3. DISSEMINATION AND VALORISATION

- Our spectra have been sent to colleagues from **University of Bremen** (T. Warneke, M. Buschmann, and R. Chiarella), as part of the European project C3S-BARON. Our partners will performed **CO_2 retrievals** based on our Porto Velho spectra, and the spectra from their own stations (Bremen, Ny-Alesund, Paramaribo). Our station is an important site in their study because they want to optimize a retrieval strategy for CO_2 that will perform well for sites operating at very different conditions (humidity – i.e. weak/strong interference with water vapor lines; and CO_2 emissions). **Once the settings are optimized for this set of different stations, it will be proposed as a harmonized retrieval strategy for the whole NDACC IRWG community.**

- In addition to the IKARE species, we have retrieved the official NDACC species **CH_4 and N_2O**. These 2 species time-series, **in addition to the CO** one, have been provided to our partner Carlos Aquino (**IFRO**) and his colleagues Luciana Gatti (**INPE**, Sao Paulo) and Cristiane Silvestrini de Morais (IFRO) for a collaboration on a project about greenhouse gases measurements over Brazil. Our FTIR data are compared to aircraft data and will be part of the PhD thesis of Carlos Aquino.
  The results of this collaboration will be presented at:
  - 20th WMO / IAEA Meeting on Carbon Dioxide, Other Greenhouse Gases, and Related Measurement Techniques (GGMT-2019), Jeju, Republic of Korea from 2-5 September 2019.

- All our retrieved species at Porto Velho (the **IKARE species + the greenhouse gases CH_4 and N_2O + OCS**) has been presented in international meetings:

  - Vigouroux, C., et al.: FTIR measurements at Porto Velho, oral presentation, CARBAM First meeting, Sao Paulo, 21-22 Feb., 2018.
  - Sha, M. et al.: BIRA-IASB site report, oral presentation, IRWG annual meeting, Paris, 29 May - 2 Jun., 2017.

- Our **HCHO** data at Porto Velho has been shown in several meetings (and in one publication, see Sect. 5):

  - Vigouroux, C., et al.: Harmonization of HCHO products from NDACC solar absorption FTIR measurements in view of satellite and model validation, oral presentation, TROPOMI/S5P internal workshop, Brussels, 17th Oct., 2017.
  - Vigouroux, C., et al.: Harmonization of HCHO products from NDACC solar absorption FTIR measurements in view of satellite and model validation, oral presentation, IRWG annual meeting, Paris, 29 May - 2 June, 2017.

  - Vigouroux, C., et al.: Harmonization of HCHO products from NDACC solar absorption FTIR measurements in view of satellite and model validation, oral presentation, ESRIN, 18-20 Oct., 2016.

- Our **HCHO** data at Porto Velho are now used for the validation of **TROPOMI** data and the results will be shown in the next ESA Validation meeting, ESRIN, 11-14 Nov. 2019.

- Our **HCHO** data at Porto Velho are used by **other BIRA teams**:
  - For the **GOME-2 validation**: Pinardi, G. et al.: Validation of the GOME-2 AC SAF GDP HCHO columns using ground-based MAXDOAS and FTIR column measurements, oral presentation, EUMETSAT conference, Tallinn, 17-21 Sept., 2018.
  - For the comparison with the **IMAGES model after inversion of OMI data**: Bauwens et al.: Thirteen years of top-down VOC emission estimates over South America inferred by inversion of OMI formaldehyde observations, poster presentation, EGU conference, Vienna, 7-12 April 2019.

4. PERSPECTIVES

- **Our longer-term perspective for IKARE was to start long-term monitoring at Porto Velho and to certify this site as a new NDACC station**, for increasing the spatial coverage and significance of the network and the role of BIRA-ISAB at the international level. We have the instrument running in the complete configuration, required for a NDACC station, since June 2019 (Task 1.1), and we retrieve with success the main official NDACC species**. Therefore, we believe that our Porto Velho station can become an NDACC site in 2020, or 2021 at the latest.**

- We plan to **continue the successful collaboration with our partner IFRO**. While we benefit from the local help of Carlos Aquino and Christiane Silivistrini de Morais for the instrumental issues, we share our strong knowledge acquired at BIRA-IASB about FTIR measurements and validation. We share our retrieved time-series for the IFRO and INPE projects on greenhouse gases. In addition to the current work on CH_4 and CO, we will share our CO2 data as soon as we will have them as output of the C3S-BARON project.

- Our **HCHO** data at Porto Velho has been extensively used for the validation of TROPOMI, GOME-2 and OMI, as well as for modeling studies. These different works are **planned to be published in the coming months.**

- Our **CO data will be used for the TROPOMI validation** (M. Sha and B. Langerock, BIRA-IASB), within the TROVA-2 project.

- When at least one more biomass burning season data will become available (in the next coming months):
    - IMAGES model sensitivity studies should be carried on to finalized our results on emissions factors.
    - As soon as GFEDv4.1 will update its preliminary emission estimates, Flexpart simulations will be revisited with a clear perspective to gain information on the emission fractions

- **Our comparisons with IASI data (C_2H_2, CH_3OH and HCOOH) should continue (if funding is found)**, to better understand the observed disagreement and study how either IASI data can be improved or how the IMAGES model could take into account the high IASI observed bias when using it in inverse modeling, **in order to obtain not biased a posteriori emissions.**

- More generally, we believe that FTIR measurements could be used in inversion studies: the satellite known bias could be corrected prior to its inversion by models to avoid to have underestimated emissions in the model, especially when a network of FTIR stations are used to consolidate the validation results, as it is the case for OMI and TROMOPI HCHO validation.

5. PUBLICATIONS

Vigouroux, C., Bauer Aquino, C. A., Bauwens, M., Becker, C., Blumenstock, T., De Mazière, M., García, O., Grutter, M., Guarin, C., Hannigan, J., Hase, F., Jones, N., Kivi, R., Koshelev, D., Langerock, B., Lutsch, E., Makarova, M., Metzger, J.-M., Müller, J.-F., Notholt, J., Ortega, I., Palm, M., Paton-Walsh, C., Poberovskii, A., Rettinger, M., Robinson, J., Smale, D., Stavrakou, T., Stremme, W., Strong, K., Sussmann, R., Té, Y., and Toon, G.: **NDACC harmonized formaldehyde time series from 21 FTIR stations covering a wide range of column abundances**, Atmos. Meas. Tech., 11, 5049-5073, https://doi.org/10.5194/amt-11-5049-2018, 2018.

Sun, Y., Liu, C., Palm, M., **Vigouroux, C.,** Notholt, J., Hu, Q., Jones, N., Wang, W., Su, W., Zhang, W., Shan, C., Tian, Y., Xu, X., De Mazière, M., Zhou, M., and Liu, J.: Ozone seasonal evolution and photochemical production regime in the polluted troposphere in eastern China derived from high-resolution Fourier transform spectrometry (FTS) observations, Atmos. Chem. Phys., 18, 14569-14583, https://doi.org/10.5194/acp-18-14569-2018, 2018. (Our co-auhorship in this paper is due to our work on **our optimization of HCHO** retrieval settings).

6. ACKNOWLEDGEMENTS

Part of our work (HCHO optimized retrieval strategy and TROPOMI validation) has also been funded by the projects TROVA and TROVA-2.

7. REFERENCES

WEB 2019: Web references in the media concerning the August 2019 fires in Amazonia:

- BBC News, 21st August 2019: https://www.bbc.com/news/world-latin-america-49415973

- The Guardian, 23rd August 2019: https://www.theguardian.com/environment/2019/aug/23/amazon-fires-global-leaders-urged-divert-brazil-suicide-path

- CNN, 23rd August 2019: https://edition.cnn.com/americas/live-news/amazon-wildfire-august-2019/index.html

- Libération, 27th Agust 2019:
- https://www.liberation.fr/checknews/2019/08/27/l-ampleur-des-incendies-en-amazonie-est-elle-vraiment-historique_1747356

- Copernicus & ESA communication : https://twitter.com/copernicuseu/status/1164190830816583680

  http://www.esa.int/Our_Activities/Observing_the_Earth/Copernicus/Sentinel-5P/Monitoring_air_pollution_from_fires?f

Andreae, M. O. and Merlet, P.: Emission of trace gases and aerosols from biomass burning, Global Biogeochem. Cy., 15, 955–966,2001.

Andreae, M. O.: Emission of trace gases and aerosols from biomass burning – an updated assessment, Atmos. Chem. Phys., 19, 8523-8546, https://doi.org/10.5194/acp-19-8523-2019, 2019.

Barkley, M. P., De Smedt, I., Van Roozendael, M., Kurosu, T.M., Chance, K., Arneth, A., Hagberg, D., Guenther, A., Paulot, F., Marais, E., and Mao, J. (2013): Top-down isoprene emissions over tropical South America inferred from SCIAMACHY and OMI formaldehyde columns, J. Geophys. Res. Atmos., 118, 6849–6868, doi:10.1002/jgrd.50552, 2013.

Bauwens, M., Stavrakou, T., Müller, J.-F., De Smedt, I., VanRoozendael, M., van der Werf, G. R., Wiedinmyer, C., Kaiser,J. W., Sindelarova, K., and Guenther, A.: Nine years of globalhydrocarbon emissions based on source inversion of OMIformaldehyde observations, Atmos. Chem. Phys., 16, 10133–10158, https://doi.org/10.5194/acp-16-10133-2016, 2016.

Bey, I., Jacob, D. J., Yantosca, R. M., Logan, J. A., Field,B. D., Fiore, A. M., Li, Q. B., Liu, H. G. Y., Mickley,L. J., and Schultz, M. G.: Global modeling of tropospherichemistry with assimilated meteorology: Model descriptionand evaluation, J. Geophys. Res.-Atmos., 106, 23073–23095,doi:10.1029/2001JD000807, 2001.

De Smedt, I., Stavrakou, T., Hendrick, F., Danckaert, T., Vlemmix, T., Pinardi, G., Theys, N., Lerot, C., Gielen, C, Vigouroux, C., Hermans, C., Fayt, C., Veefkind, P., Müller, J.-F., and Van Roozendael, M: Diurnal, seasonal and long-term variations of global formaldehyde columns inferred from combined OMI and GOME-2 observations, submitted to ACP, 2015.

De Smedt, I., Theys, N., Yu, H., Danckaert, T., Lerot, C., Compernolle, S., Van Roozendael, M., Richter, A., Hilboll, A., Peters, E., Pedergnana, M., Loyola, D., Beirle, S., Wagner, T., Eskes, H., van Geffen, J., Boersma, K. F., and Veefkind, P.: Algorithm theoretical baseline for formaldehyde retrievals from S5P TROPOMI and from the QA4ECV project, Atmos. Meas. Tech., 11, 2395-2426, https://doi.org/10.5194/amt-11-2395-2018, 2018.

Dentener, F., Kinne, S., Bond, T., Boucher, O., Cofala, J., Generoso, S., Ginoux, P., Gong, S., Hoelzemann, J. J., Ito, A., Marelli, L., Penner, J. E., Putaud, J.-P., Textor, C., Schulz, M., van der Werf, G. R., and Wilson, J.: Emissions of primary aerosol and precursor gases in the years 2000 and 1750 prescribed data-sets for AeroCom, Atmos. Chem. Phys., 6, 4321-4344, https://doi.org/10.5194/acp-6-4321-2006, 2006.

Duflot, V., Wespes, C., Clarisse, L., Hurtmans, D., Ngadi, Y., Jones, N., Paton-Walsh, C., Hadji-Lazaro, J., Vigouroux, C., De Mazière, M., Metzger, J.-M., Mahieu, E., Servais, C., Hase, F., Schneider, M., Clerbaux, C., and Coheur, P.-F.: Acetylene (C2H2) and hydrogen cyanide (HCN) from IASI satellite observations: global distributions, validation, and comparison with model, Atmos. Chem. Phys., 15, 10509-10527, https://doi.org/10.5194/acp-15-10509-2015, 2015.

Eerdekens, G., Ganzeveld, L., Vilà-Guerau de Arellano, J., Klüpfel, T., Sinha, V., Yassaa, N., Williams, J., Harder, H., Kubistin, D., Martinez, M., and Lelieveld, J.: Flux estimates of isoprene, methanol and acetone from airborne PTR-MS measurements over the tropical rainforest during the GABRIEL 2005 campaign, Atmos. Chem. Phys., 9, 4207-4227, https://doi.org/10.5194/acp-9-4207-2009, 2009.

Franco, B., Clarisse, L., Stavrakou, T., Müller, J.-F., Van Damme, M., Whitburn, S., Hadji-Lazaro, J., Hurtmans, D., Taraborrelli, D., Clerbaux, C., and Coheur, P.-F.: A general framework for global retrievals of trace gases from IASI: Application to methanol, formic acid, and PAN. Journal of Geophysical Research: Atmospheres, 123, 13,963– 13,984, https://doi.org/10.1029/2018JD029633, 2018.

George, M., Clerbaux, C., Bouarar, I., Coheur, P.-F., Deeter, M. N., Edwards, D. P., Francis, G., Gille, J. C., Hadji-Lazaro, J., Hurtmans, D., Inness, A., Mao, D., and Worden, H. M.: An examination of the long-term CO records from MOPITT and IASI: comparison of retrieval methodology, Atmos. Meas. Tech., 8, 4313-4328, https://doi.org/10.5194/amt-8-4313-2015, 2015.

Hornbrook, R. S., Blake, D. R., Diskin, G. S., Fried, A., Fuelberg, H. E., Meinardi, S., Mikoviny, T., Richter, D., Sachse, G. W., Vay, S. A., Walega, J., Weibring, P., Weinheimer, A. J., Wiedinmyer, C., Wisthaler, A., Hills, A., Riemer, D. D., and Apel, E. C.: Observations of nonmethane organic compounds during ARCTAS – Part 1: Biomass burning emissions and plume enhancements, Atmos. Chem. Phys., 11, 11103-11130, https://doi.org/10.5194/acp-11-11103-2011, 2011.

Keppel-Aleks, Gretchen, Geoffrey Toon, Paul Wennberg, and Nicholas Deutscher, "Reducing the impact of source brightness fluctuations on spectra obtained by FTS", Applied Optics, 46, 4774-4779, 2007.

Kuhn, U., Rottenberger, S., Biesenthal, T., Ammann, C., Wolf, A.,Schebeske, G., Oliva, S. T., Tavares, T. M., and Kesselmeier, J.: Exchange of short-chain monocarboxylic acids by vegetation at a remote tropical forest site in Amazonia, J. Geophys. Res., 107, 8069, doi:10.1029/2000JD000303, 2002.

Neefs, E., De Mazière, M., Scolas, F., Hermans, C., and Hawat, T. : BARCOS, an automation and remote control system for atmospheric observations with a Bruker interferometer, Review of Scientific Instruments, 78, 035109 (2007), doi: 10.1063/1.2437144, 2007.

Paulot, F., Wunch, D., Crounse, J. D., Toon, G. C., Millet, D. B., DeCarlo, P. F., Vigouroux, C., Deutscher, N. M., González Abad, G., Notholt, J., Warneke, T., Hannigan, J. W., Warneke, C., de Gouw, J. A., Dunlea, E. J., De Mazière, M., Griffith, D. W. T., Bernath, P., Jimenez, J. L., and Wennberg, P. O.: Importance of secondary sources in the atmospheric budgets of formic and acetic acids, Atmos. Chem. Phys., 11, 1989-2013, 2011.

Rodgers, C. D.: Inverse Methods for Atmospheric Sounding: Theory and Practice, World Scientific Publishing Co. Pte. Ltd, New Jersey, 2000.

Rodgers, C. D. and Connor, B. J.: Intercomparison of remote sound-ing instruments, J. Geophys. Res. 108, 4116–4129, 2003.

Senten, C., De Mazière, M., Dils, B., Hermans, C., Kruglanski, M., Neefs, E., Scolas, F., Vandaele, A.-C., Vanhaelewyn, G., Vigouroux, C., Carleer, M., Coheur, P.-F., Fally, S., Barret, B., Baray, J.-L., Delmas, R., Leveau, J., Metzger, J.-M., Mahieu, M., Boone, C., Walker, K. A., Bernath, P. F., and Strong K.: Technical Note: New ground-based FTIR measurements at Ile de La Réunion: observations, error analysis, and comparisons with independent data, ACP, 8, 3483-3508, 2008.

Stavrakou, T., Guenther, A., Razavi, A., Clarisse, L., Clerbaux, C., Coheur, P.-F., Hurtmans, D., Karagulian, F., De Mazière, M., Vigouroux, C., Amelynck, C., Schoon, N., Laffineur, Q., Heinesch, B., Aubinet, M., Rinsland, C., and Müller, J.-F.: First space-based derivation of the global atmospheric methanol emission fluxes, Atmos. Chem. Phys., 11, 4873-4898, 2011.

Sofiev, M., Ermakova, T., and Vankevich, R.: Evaluation of the smoke-injection height from wild-land fires using remote-sensing data, Atmos. Chem. Phys., 12, 1995-2006, https://doi.org/10.5194/acp-12-1995-2012, 2012.

Stavrakou, T., Müller, J.-F., Peeters, J., Razavi, A., Clarisse, L., Clerbaux, C., Coheur, P.-F., Hurtmans, D., De Mazière, M., Vigouroux, C., Deutscher, N. M., Griffith, D. W. T. , Jones N., and Paton-Walsh, C.: Satellite evidence for a large source of formic acid from boreal and tropical forests, Nature Geosci., 5, 26-30, 2012.

Stohl, A., Forster, C., Frank, A., Seibert, P., and Wotawa, G.: Technical note: The Lagrangian particle dispersion model FLEXPART version 6.2, Atmos. Chem. Phys., 5, 2461-2474, https://doi.org/10.5194/acp-5-2461-2005, 2005

Stone, T.A., P. Schlesinger, G.M. Woodwell, and R.A. Houghton, 1994. A Map of the Vegetation of South America Based on Satellite Imagery. Photogrammetric Engineering and Remote Sensing. 60(5):541-551.

Sun, Y., Liu, C., Palm, M., **Vigouroux, C.,** Notholt, J., Hu, Q., Jones, N., Wang, W., Su, W., Zhang, W., Shan, C., Tian, Y., Xu, X., De Mazière, M., Zhou, M., and Liu, J.: Ozone seasonal evolution and photochemical production regime in the polluted troposphere in eastern China derived from high-resolution Fourier transform spectrometry (FTS) observations, Atmos. Chem. Phys., 18, 14569-14583, https://doi.org/10.5194/acp-18-14569-2018, 2018.

Vigouroux, C., Hendrick, F., Stavrakou, T., Dils, B., De Smedt, I., Hermans, C., Merlaud, A., Scolas, F., Senten, C., Vanhaelewyn, G., Fally, S., Carleer, M., Metzger, J.-M., Müller, J.-F., Van Roozendael, M., and De Mazière, M.: Ground-based FTIR and MAX-DOAS observations

of formaldehyde at Réunion Island and comparisons with satellite and model data, Atmos. Chem. Phys., 9, 9523-9544, 2009.

Vigouroux, C., T. Stavrakou, C. Whaley, B. Dils, V. Duflot, C. Hermans, N. Kumps, J.-M. Metzger, F. Scolas, G. Vanhaelewyn, J.-F. Müller, D. B. A. Jones, Q. Li, and M. De Mazière, FTIR time-series of biomass burning products (HCN, C2H6, C2H2, CH3OH, and HCOOH) at Reunion Island (21°S, 55°E) and comparisons with model data, Atmos. Chem. Phys., 12, 10367-10385, doi:10.5194/acp-12-10367-2012, 2012.

Vigouroux, C., Bauer Aquino, C. A., Bauwens, M., Becker, C., Blumenstock, T., De Mazière, M., García, O., Grutter, M., Guarin, C., Hannigan, J., Hase, F., Jones, N., Kivi, R., Koshelev, D., Langerock, B., Lutsch, E., Makarova, M., Metzger, J.-M., Müller, J.-F., Notholt, J., Ortega, I., Palm, M., Paton-Walsh, C., Poberovskii, A., Rettinger, M., Robinson, J., Smale, D., Stavrakou, T., Stremme, W., Strong, K., Sussmann, R., Té, Y., and Toon, G.: NDACC harmonized formaldehyde time series from 21 FTIR stations covering a wide range of column abundances, Atmos. Meas. Tech., 11, 5049-5073, https://doi.org/10.5194/amt-11-5049-2018, 2018.

ANNEXES